Ozone in the Pacific Tropical Troposphere From Ozonesonde Observations

S.J. Oltmans[1], B.J. Johnson[1], J.M. Harris[1], H. Vömel[1,2], K. Koshy[3], P. Simon,[4], R. Bendura[5], A.M. Thompson[6], J.A. Logan[7], F. Hasebe[8], M. Shiotani[9], M. Maata[3], G. Sami[3], A. Samad[3], J. Tabuadravu[3], H. Enriquez[10], M. Agama[11], J. Cornejo[11], and F. Paredes[11]

[1] NOAA, Climate Monitoring and Diagnostics Laboratory (CMDL), Boulder, CO 80305, USA

[2] Cooperative Institute for Research in the Environmental Sciences (CIRES), University of Colorado, Boulder, CO, 80309, USA

[3] University of the South Pacific, Suva, Fiji

[4] MeteoFrance, Papeete, Tahiti, French Polynesia

[5] NASA, Langley Research Center, Hampton, VA, USA

[6] NASA, Goddard Space Flight Center, Greenbelt, MD, USA

[7] Harvard University, Cambridge, MA, USA

[8] Ibaraki University, Mito, Japan

[9] Hokkaido University, Sapporo, Japan

[10] INAMHI, Quito, Ecuador

[11] INAMHI, San Cristobal, Galapagos, Ecuador

ABSTRACT: Ozone vertical profile measurements obtained from ozonesondes flown at Fiji, Samoa, Tahiti and the Galapagos are used to characterize ozone in the troposphere over the tropical Pacific. There is a significant seasonal variation at each of these sites. At sites in both the eastern and western Pacific, ozone is highest at almost all levels in the troposphere during the September-November season and lowest during March-May. There is a relative maximum at all of the sites in the mid-troposphere during all seasons of the year (the largest amounts are usually found near the tropopause). This maximum is particularly pronounced during the September-November season. On average, throughout the troposphere at all seasons, the Galapagos has larger ozone amounts than the western

Pacific sites. A trajectory climatology is used to identify the major flow regimes that are associated with the characteristic ozone behavior at various altitudes and seasons. The enhanced ozone seen in the mid-troposphere during September-November is associated with flow from the continents. In the western Pacific this flow is usually from southern Africa (although 10-day trajectories do not always reach the continent), but also may come from Australia and Indonesia. In the Galapagos the ozone peak in the mid-troposphere is seen in flow from the South American continent and particularly from northern Brazil. The time of year and flow characteristics associated with the ozone mixing ratio peaks seen in both the western and eastern Pacific suggest that these enhanced ozone values result from biomass burning. In the upper troposphere low ozone amounts are seen with flow that originates in the convective western Pacific.

Introduction

The tropical Pacific is often considered to be a region remote from major polluting influences because of its isolation from heavily industrialized landmasses. Recent field campaigns (Hoell et al., 1999) have emphasized that though this is often the case, the signature of pollution, particularly from biomass burning, makes a significant imprint on the air chemistry of the region. In a number of instances layers of enhanced ozone (mixing ratios >80 ppbv) were found in the mid-troposphere in the remote western Pacific (Stoller, et al., 1999). These layers in addition to having enhanced ozone were replete with markers of biomass burning (Gregory et al.,1999).

Beginning in August 1995 as part of the Pacific Exploratory Mission (PEM) Tropics A, ozone vertical profile measurements were started at Pago Pago, American Samoa (14.3S, 170.6W) and Papeete, Tahiti (18.0S, 149.0W). At Samoa profiles were also obtained as part of an earlier measurement program from 1986-1989. These earlier profiles provide an opportunity for comparison with measurements during the more recent period. Profile measurements were continued at Tahiti and Samoa through PEM Tropics B with the program at Tahiti completed in December 1999. At Samoa weekly soundings continue as part of the Southern Hemisphere Additional Ozonesondes (SHADOZ) project. During most of the measurement period soundings were done weekly. During the aircraft field campaigns in September-October 1996 (PEM Tropics A) and March-April 1999 (PEM Tropics B) soundings were done twice a week. In January 1997 weekly soundings were begun at Suva, Fiji (18.1S, 178.2E) in anticipation of PEM Tropics B. As part of the Soundings of Ozone and Water Vapor in the Equatorial Region (SOWER) project ozone profile measurements were started on a campaign basis in March 1998 at San Cristobal, Galapgos (0.9S, 89.6W), were increased to bi-weekly soundings in September 1998, and to weekly soundings as part of SHADOZ early in 1999. Soundings continue at Fiji and the Galapagos in 2000 as part of SHADOZ and SOWER.

This set of ozone profiles obtained using balloon-borne ozonesondes provides information on the distribution of ozone throughout the troposphere of the tropical Pacific that has not been available in the past. In particular, new insights on the short-term and seasonal variability of ozone in this region as well as differences between the eastern and western Pacific can be gleaned from these data. In addition, isentropic trajectories are

used to look at the transport associated with particular features of individual profiles, and also at the influence of climatological transport patterns on the principle features of the ozone distribution in the tropical troposphere in this region.

Methods

Ozonesondes

The ozone vertical profiles were obtained using the electrochemical concentration cell (ECC) ozonesonde (Komhyr et al., 1995). This has become a standard technique for obtaining ozone profiles with high vertical resolution in both the troposphere and stratosphere to altitudes of approximately 35 km. The measurements of ozone have an accuracy of ±5% through most of the troposphere with somewhat poorer performance (±10%) for very low mixing ratios (<10 ppbv) encountered occasionally in the tropics. The only important interferent in the measurement technique, which is based on the oxidation reaction of ozone with potassium iodide in solution, is sulfur dioxide that is not encountered at these sites at sufficient concentrations to be of significance. The data were obtained with an altitude resolution of about 50 m but for the analysis performed here were averaged into 250 m layers. Only at Samoa are total column ozone measurements from a collocated Dobson spectrophotometer available for comparison with the integrated total ozone from the ozonesonde. These comparisons give an average ratio of 1.03 ± 0.05 between the Dobson total ozone measurement and the integrated total ozone from the ozonesonde, giving confidence that the ozonesonde measured ozone amounts from all of the sites can be compared with each other. During the course of the measurement program a change was made in early 1998 in the sensing solution recipe (Johnson et al.,

2000) at all of the sites except the Galapagos where the new recipe was used from the beginning. This change primarily affects the measurements in the stratosphere. From comparison flights made at these sites, as well as laboratory tests, an empirical correction has been derived, and the earlier data have been corrected using this relationship. Data archived in the Global Troposhere Experiment (GTE) archive for PEM Tropics at NASA Langley have this correction applied.

Trajectories

For the purposes of characterizing the tropospheric air-flow patterns influencing transport to the tropical sites, insentropic trajectories have been calculated. The trajectories are computed from the ECMWF analyses using the model described in Harris and Kahl (1994). The limitations in such trajectories must be recognized in interpreting the results that are obtained, but they do provide a useful tool for obtaining a picture of the flow patterns that may influence ozone behavior at these sites. The computed trajectories are used both to investigate individual cases, and by grouping the trajectories using an objective clustering technique (Moody, 1986; Harris and Kahl, 1990) that gives an indication of the primary flow regimes influencing a particular location at a given altitude. The trajectories are computed twice daily (00 and 12 UT) for 10 days backward in time. Air parcels reaching a site after 10 days of travel may have undergone diabatic processes that are not accounted for in the model used here, and these are an important contribution to the uncertainty in the computed pathway of the air parcel (Merrill, 1996). Transport from sources or sinks more than 10 days travel time from a particular site could also have a significant influence on ozone levels measured at the site.

Day-to-day variations

Variations on the order of several days are a large source of the variability seen in tropospheric ozone at the Pacific tropical sites studied here as will be shown in the analysis in this section. These variations have been studied from surface observations at Samoa (Harris and Oltmans, 1998). The surface variations were found to result from changes in airflow to the site that tapped different sources and sinks. During all seasons air coming from higher latitudes and altitudes has about 50% more ozone than air with a tropical origin (Harris and Oltmans, 1998). Although the ozone soundings are done on an approximately weekly schedule compared to the continuous observations at the surface, the variability from sounding-to-sounding captured in the time-height cross-section of ozone mixing ratio for 1996 at Samoa (Plate 1) is also apparent. During 1996 at Samoa the soundings were done twice a week during September and October so that the variability is well represented during this time of the year. This can also be seen in the plot of the average profiles at 0.25 km increments for individual seasons at Tahiti (Figure 1). The median is the horizontal line inside of the box, and the box represents the inner 50^{th} percentile of the data. The whiskers represent the inner 90^{th} percentile of the data. The solid diamond is the mean. The September-November period has greatly enhanced variability especially in the 2-10km layer when compared to the March-May period. These seasonal profiles are based on several years of data, and represent the variability that is primarily contributed by the short-term fluctuations within a season.

In the Galapagos the time-height cross-section for 1999 (Plate 2), the only complete year available for this site, shows many of the same features seen at Samoa. The seasonal profiles for the Galapagos (figure 2) show similar behavior to Tahiti with a maximum in the variability in September-November and a minimum in the March-May season. The variability is greater at Tahiti in September-November than it is in the Galapagos. At Samoa (Figure 3) the variability in this season is also larger than at the Galapagos but not quite as large as at Tahiti. Since Fiji (Figure 4) also shows greater variability during this season, the larger variability is likely a real difference between the eastern and western Pacific.

Seasonal variation

As can be seen in figures 1 - 4, not only is the variability of ozone in the troposphere greater in September-November than in March-May, but also the mean (and the median) values are greater as well. Time-height cross-sections based on 14-day averages over the entire record of measurements (which varies somewhat for each site) are shown in plate 3. Although there are unique features at each site, a pattern is discernable that is reflected at all sites. In the western Pacific there is a prominent layer of enhanced ozone in the mid-troposphere in September and October. There also seems to be a distinct pulse in June and July of somewhat smaller magnitude with a relative minimum in late July and August. Associated with this June-July enhancement in the mid-troposphere, ozone in the boundary layer also increases and this produces a seasonal maximum near the surface that occurs earlier than the peak in the mid-troposphere. During austral winter and spring higher ozone amounts descend to about 10-12 km giving higher ozone in the upper

troposphere. This seems to be associated with ozone in the lower stratosphere. In January-May ozone at all latitudes is almost always lower than at a corresponding altitude during the rest of the year. Also at this time of year ozone in the upper troposphere is often very low with amounts approaching those seen at the surface which are almost always quite low (<15 ppbv) in this season.

An earlier set of profiles obtained at Samoa from August 1986 – January 1990 (Figure 5) show similar characteristics to those seen in the more recent 5-year data set. For March-May the earlier period has somewhat more ozone that appears to be driven by several profiles with greater ozone amounts, particularly in the low and mid-troposphere (Figure 5a). In September-November, however, the amounts and variability are very similar (Figure 5b).

In the Galapagos the general picture is similar to the western Pacific sites, but with some important differences (Figure 6). The mid-tropospheric ozone maximum occurs earlier in the year and diminishes earlier as well. Near the surface the seasonal variation is smaller. The most noticeable difference is the lack of very low mixing ratios in the middle and upper troposphere especially during the January-May time of year. This is consistent with the fact that the western Pacific is a more convective region where boundary layer air can be mixed into the upper troposphere. Other than this noticeable lack of low ozone amounts the differences among the western Pacific sites is similar to the difference between the eastern and western Pacific. It is also clear that in the Galapagos ozone

amounts are greater than in the western Pacific above 4 km in September-November and above 5 km in March-May .

Flow characteristics

Although the seasonal ozone behavior at all of the sites has some features in common such as the maximum during the austral spring (September-November), this does not by itself imply that the sources and sinks influencing the measured ozone at the sites are the same. For example the proximity of the Galapagos to the South American continent suggests that this continent is more likely to have a greater influence on this site than the western Pacific. The following analysis shows that while the airflow patterns at the western Pacific sites are quite similar, they are much different from those in the Galapagos. The differences in airflow direction with season are greatest in the boundary layer and somewhat greater at all levels in the Galapagos than in the western Pacific. To carry out this analysis a 10-year climatology of 10-day back trajectories was computed at three levels (1, 6, and 13 km) for all four of the sites for each of four seasons. These trajectories were grouped into six clusters at each site for each altitude. Examples representative of various regimes are discussed here (Figures 7-12).

Because of the similarity in flow patterns at the western Pacific sites the description of the behavior at Tahiti is used to indicate the overall pattern with some differences from the other sites noted. At 1 km, a level in the marine boundary layer, the largest seasonal contrast is between December-February (Figure 7a) and June-August (Figure 7b). These are the seasons of minimum and maximum surface ozone at Samoa (Harris and Oltmans,

1997). During the austral summer (Dec.-Feb.) flow at this level is predominantly from the tropical Pacific for all of the sites in the western Pacific. In the other seasons 15-65% of the flow is from the west and more southerly latitudes with the largest percentage of flow from the south occurring in austral winter. Fiji shows this most prominently with 65% of the trajectories coming from the south and west during June-August while at Tahiti and Samoa the percentage of southerly flow is closer to 30% (Figure 7b).

At 6 km at Tahiti flow (Figure 8) is more uniformly from the west with only about 20% coming from the east on an annual basis. There is a southerly component to the airflow but it usually does not extend south of 40S within 10 days, in contrast to the low level flow that reaches much higher latitudes. Throughout the austral winter and spring (June-November) at least 25% of the trajectories arriving at Tahiti come from as far west as the mid Indian Ocean and about 10% reach southern Africa (Figure 8b) within 10 days. To Fiji the flow is even more vigorous from the west and about 5% of the trajectories come from South America. A number of trajectories also have their 10-day origins over northern Australia. In the summer flow is less vigorous and some trajectories have a northerly component.

In the upper troposphere (13 km) the flow is from the west but a majority of the trajectories also have a northerly component (Figure 9). This northerly flow brings air from near or even north of the equator and is strongest in September-November but is present in other seasons as well. As in the mid-troposphere, a significant number of the trajectories come from the Indian Ocean and Africa.

The flow patterns in the Galapagos differ significantly from those in the western Pacific. At the lowest level (Figure 10) the flow is overwhelmingly from the south and over the ocean in all seasons. There is some variation with season with December-May showing 10-15% of the trajectories coming from the Atlantic. In June-November the flow is exclusively from the south, often paralleling the South American coast. The flow at 6 km is in strong contrast to that in the boundary layer. On an annual basis 75% of the trajectories arrive at San Cristobal from the east and have passed over the South American continent in the previous 10 days. In December-February (Figure 11a) about 10% of trajectories arrive from the tropical north Pacific, another 10% from the tropical south Pacific, and the remainder from the east off continental South America. During June-November (June-August shown in Figure 11b) about 10-15% of the flow is from the tropical south Pacific with the remainder from the east or with little movement (cluster 3 in figure 11b). At 13 km (Figure 12) the flow is about equally divided into weak flow from the east or northeast and vigorous flow from the west. There is a fairly strong seasonality with December-May dominated by trajectories arriving from the west, but about half the trajectories during June-November come from the east and northeast.

Discussion

In the previous sections the day-to-day and seasonal variations have been described as well as the major air flow characteristics affecting the ozonesonde sites in the western and eastern tropical Pacific. In this section important features of the ozone profile are linked to the trajectories to show how important source and sink regions for ozone may

contribute to both the shorter term and seasonal variations. Since the tropics are known to be a significant area of biomass burning (see TRACE-A and SAFARI Special Issue of the *Journal of Geophysical Research, 101*, 1996) particular attention is paid to characterizing the possible influence of burning on ozone at these sites by linking enhanced ozone layers with flow from potential source regions. It appears that several burning regions contribute to what is seen at these sites. The low ozone mixing ratios seen in the upper troposphere at the western Pacific sites are also briefly discussed.

It is clearly seen from Plate 3 that there is a persistent layer of enhanced ozone in the mid-troposphere in the June-November season. The climitological trajectory analysis also shows this season to be one of regular occurrences of flow from potential burning related source regions in southern Africa and Australia for the western locations and South America for San Cristobal. Several individual profiles are examined that contain enhanced mid-tropospheric ozone along with the trajectories calculated for these cases. Profiles that show little or no ozone enhancement are also examined in relation to flow characteristics. An event of very high ozone seen at Fiji and Samoa in November 1997 is investigated because the flow path suggests an Indonesian source for the enhanced ozone.

A profile with an enhanced mid-tropospheric layer characteristic of those seen during the September and October period in the western Pacific is shown in figure 13 for a sounding done at Samoa on October 30, 1998. The peak ozone mixing ratio of 105 ppbv at ~6 km has a trajectory (Figure 14) that reaches back to southern Africa 10 days prior to the sounding. Ozone profiles with peaks greater than about 70 ppbv (Figure 15) do not

always have trajectories (Figure 16) that extend back to Africa in 10 days, but they always have paths that have a strong westerly component that goes to the west of Australia into the Indian Ocean. On many occasions the trajectories pass over Australia, usually through the middle or southern part of the continent. The marked contrast that can occur during a month (see figure 13) illustrates the dominant role that the airflow (Figure 16) to a particular site plays in the ozone profile, particularly during this season. For the profile obtained on October 30, 1997 the 10-day trajectory (Figure 16b) in the mid-troposphere shows little air movement from the vicinity of Samoa and mixing ratios are 20-25 ppmv or less throughout the troposphere.

From figure 8 it is clear that a large fraction of the air parcels reaching Tahiti (and also Samoa and Fiji) pass over Australia. From the data that are available from the ozonesondes and trajectories it is difficult to determine if trajectories that pass over Australia may be influenced by burning in Australia rather than southern Africa (Olson et al., 1999). In some cases the trajectories show that the air moves more slowly (for example cluster 3 in figure 8b). An example of such a case is shown in the profile of October 31, 1995 at Tahiti (Figure 17). The corresponding trajectory just reaches the York Peninsula of Australia (Figure 18) in 10 days. The relatively slow transport, the large peak mixing ratio, and the thin vertical extent of the layer suggest that the source of the elevated ozone seen at Tahiti may have been relatively nearby (i.e., Australia rather than southern Africa).

In 1997 extensive burning took place in Indonesia associated with drought conditions that were a consequence of the strong El Nino. Ozone profile measurements over the Indonesian region have shown high ozone was found in Indonesia and Malaysia in connection with the burning in the region (Fujiwara et al., 1999). On November 19 and 20 at Fiji and Samoa (Figures 19) some of the highest tropospheric ozone amounts were seen for any event recorded at these sites. These enhancements, which encompassed the entire troposphere above the two sites, increased the total tropospheric column by about 20 DU, or more than 70% over average values for the month. The trajectories show that at both sites air was coming from Indonesia (Figure 20a-d) throughout the depth of the tropospheric column. Although these profiles were the only ones measured during the event, trajectories show that a flow pattern nearly identical with the one during this large ozone enhancement persisted for about 5 days around the time that the profiles were obtained (Figure 20d).

As was noted earlier, during the austral summer ozone is generally quite low throughout the troposphere in the western Pacific. Low values less than 10 ppbv are seen as in the profile for February 20, 1999 at Samoa (Figure 21) where in the 13-15 km layer ozone is about 5 ppbv. The trajectory at 13 km (Figure 22) shows that air came from northeast of Australia in a region associated with extensive convection during this time of year. The low ozone mixing ratios are not usually a result of mixing directly from the surface near the site, although surface mixing ratios are low enough. This can be seen in Plate 3a, 3c, and 3d where the minima in the upper troposphere are not connected to the low values at the surface as illustrated by the individual profile shown in figure 21. Instead there is

normally a relative maximum in the mixing ratio in the mid-troposphere. It is more likely that air with very low ozone is mixed vertically by convection in the region of northern Australia and eastern Indonesia and transported to these sites in the upper troposphere (Kley et al., 1997).

In the Galapagos many of the profiles during August-October also show pronounced mid-tropospheric peaks (Figure 23) as seen on October 9, 1999. The trajectory for this event (Figure 24) crosses Brazil in less than 10 days over a region that is heavily influenced by biomass burning during this time of the year (Fishman et al., 1996). Investigation of each profile with an enhanced ozone layer in the mid-troposphere during this time of the year showed a trajectory that passed over Brazil. At times of the year when burning is not happening in Brazil, profiles at the Galapagos do not show pronounced tropospheric peaks (Figure 25). Profiles with mixing ratios near 50 ppbv in the mid-troposphere are occasionally seen (Figure 25a). These higher amounts are generally associated with flow from continental South America (Figure 26a). However, flow from the continent may also have relatively low ozone amounts (Figures 25b and 26b). It appears that even though transport to the site is similar, that unless this flow taps a source region with higher ozone, that passing over a continent is not sufficient (although it does appear necessary) to give enhancements in the ozone amount. This was also near the end of the 1997-98 ENSO warm phase with well above normal precipitation both in the Galapagos and western equatorial South America. The profile of April 4 suggests that convection has influenced the profile since humidity is high up to about 9 km (the depression between the air temperature and frost-point temperature shown in figure 22b is small).

Conclusions

From an extensive set of ozone profiles obtained over the past several years in the tropical Pacific, a picture emerges of a region of both very low tropospheric ozone amounts (~10 ppbv) and surprisingly large (~100 ppbv) concentrations that are found at all of the sites studied. The low concentrations are expected in light of the strong photochemical sink in this region (Kley, et al., 1997), and the important role of convection, particularly during the austral summer. On the other hand the ubiquitous presence of mid-tropospheric layers of enhanced ozone demonstrates that the influence of biomass burning is widespread throughout the tropical zone during August-November. On average ozone at the equatorial Galapagos site in the eastern Pacific is greater than at the three western tropical Pacific sites. However, for individual profiles, the mid-tropospheric enhancements seen in the western Pacific attain larger mixing ratios than seen in the Galapagos. This is in spite of the fact that the Galapagos are located much closer to the potential source of burning-produced ozone in Brazil than the western Pacific sites are to the south African burning sources. The relative proximity of sources in Australia and Indonesia may, however, partially account for this. Alternatively, the much greater amount of biomass burned in southern Africa may produce larger ozone enhancements (Olson et al., 1999). The extensive burning that took place in Indonesia during the latter half of 1997 appears to have been the source of very large ozone amounts seen in Samoa and Fiji in November 1997.

References:

Fishman, J., J.M. Hoell Jr., R.D. Bendura, R.J. McNeal, V.W.J.H. Kirchhoff, NASA GTE TRACE A Experiment (September-October 1992): Overview, *J. Geophys. Res., 101*, 23,865-23,879, 1996.

Fujiwara, M., K. Kita, S. Kawakami, T. Ogawa, N. Komala, S. Saraspriya, and A. Suripto, Tropospheric ozone enhancements during the Indonesian forest fire events in 1994 and 1997 as revealed by ground-based observations, *Geophys. Res. Lett., 26*, 2417-2420, 1999.

Gregory, G.L., D.J. Westberg, M.C. Shipham, D.R. Blake, R.E. Newell, H.E. Fuelberg, R.W. Talbot, B.G. Heikes, E.L. Atlas, G.W. Sachse, B.A. Anderson, and D. C. Thornton, Chemical characteristics of Pacific tropospheric air in the region of the Intertropical Convergence Zone and South Pacific Convergence Zone, *J. Geophys. Res., 104*, 6577-5696, 1999.

Harris, J.M, and J.D. Kahl, A descriptive atmospheric transport climatology for the Mauna Loa Observatory, using clustered trajectories, *J. Geophys. Res., 99*, 13,651-13-667, 1990.

Harris, J.M. and J.D. Kahl, Analysis of 10-day isentropic flow patterns for Barrow, Alaska: 1985-1992, *J. Geophys. Res., 99*, 25,845-25855, 1994.

Harris, J.M. and S.J. Oltmans, Variations in tropospheric ozone related to transport at American Samoa, *J. Geophys. Res., 102*, 8781-8791, 1998.

Hoell, J.M, D.D. Davis, D.J. Jacob, M.O. Rogers, R.E. Newell, H.E. Fuelberg, R.J. McNeal, J.L. Raper, and R.J. Bendura, Pacific Exploratory Mission in the tropical Pacific: PEM-Tropics A, August-September 1996, *J. Geophys. Res., 104*, 5567-5583, 1999.

Johnson, B.J., S.J. Oltmans, H. Vömel, and T. Deshler, Characterization of the ECC ozonesonde, *J. Geophys. Res.*, in preparation, 2000.

Kley, D., H.G.J. Smit, H. Vömel, H. Grassl, V. Ramanathan, P.J Crutzen, S. Williams, J. Meywerk and S.J. Oltmans, Tropospheric water-vapour and ozone cross-sections in a zonal plane over the central equatorial Pacific, Q. J. R. Meteor. Soc., 123, 2009-2040, 1997.

Komhyr, W.D., R.A. Barnes, G.B. Brothers, J.A. Lathrop, and D.P. Opperman, Electrochemical concentration cell ozonesonde performance evaluation during STOIC 1989, *J. Geophys. Res., 100*, 9231-9244, 1995.

Merrill, J.T., Trajectory results and interpretation for PEM-West A, *J. Geophys. Res., 101*, 1679-1690, 1996.

Moody, J. L., *The Influence of Meteorology on Precipitation Chemistry at Selected Sites in the Eastern United States,* Ph. D. Thesis, 176pp, University of Michigan, Ann Arbor, Michigan, 1986.

Olson, J.R., B.A. Baum, D.R. Cahoon, J.H. Crawford, Frequency and distribution of forest, savanna and crop fires over tropical regions during PEM Tropics A, *J. Geophys. Res., 104*, 5865-5876, 1999.

Stoller, P., J.Y.N. Cho, R.E. Newell, V. Thomas, Y. Zhu, M.A. Carroll, G.M. Albercook, B.E. Anderson, J.D.W. Barrick, E.V. Browell, G.L. Gregory, G.W. Sachse, S. Vay, J.D. Bradshaw, and S. Sandholm, Measurement of atmospheric layers from the NASA DC-8 and P3-B aircraft during PEM-Tropics A, *J. Geophys. Res., 104*, 5745-5764, 1999.

Plate Captions:

Plate 1. Time-height cross-section of ozone mixing ratio at Pago Pago, American Samoa for 1996. Soundings are weekly except during the PEM Tropics A intensive measurement period from August-September when soundings were done twice weekly

Plate 2. Time-height cross-section of ozone mixing ratio from weekly soundings at San Cristobal, Galapagos for 1999.

Plate 3. Time-height cross-sections of ozone mixing ratio based on 14-day averages over the entire record of measurements at Samoa, Galapagos, Fiji, and Tahiti.

Figure Captions:

Figure 1. The average ozone profile and variability for 0.25 km layers at Tahiti for two seasons (March-May and September-November) for the period 1995-1999. The median is the horizontal line inside the box, and the box represents the inner 50^{th} percentile of the data. The "whiskers" represent the inner 90^{th} percentile of the data. The solid diamond is the mean.

Figure 2. Average ozone profile and variability for 0.25 km layers at Galapagos for two seasons (March-May and September-November) for the period 1998-2000.

Figure 3. Average ozone profile and variability for 0.25 km layers at Samoa for two seasons (March-May and September-November) for the period 1995-2000.

Figure 4. Average ozone profile and variability for 0.25 km layers at Fiji for two seasons (March-May and September-November) for the period 1997-2000.

Figure 5. Comparison of ozone mixing ratio profiles at Samoa from two time periods; 1986-1989 and 1995-2000 for a) March-May and b) September-November.

Figure 6. Comparison of the ozone mixing ratio profiles at Samoa and the Galapagos for March-May and September-November.

Figure 7. Clusters of trajectories arriving at Tahiti at 1 km for a) December-February and b) September-November for the period 1990-1999. The clusters are numbered 1-6 and the percentage of the total number of trajectories in each cluster is also shown.

Figure 8. Clusters of trajectories arriving at Tahiti at 6 km and for a) March-May and b) September-November.

Figure 9. Clusters of trajectories arriving at Tahiti at 13 km and for all seasons.

Figure 10. Clusters of trajectories arriving at the Galapagos at 1 km and for all seasons.

Figure 11. Clusters of trajectories arriving at the Galapagos at 6 km and for a) December –February and b) June-August.

Figure 12. Clusters of trajectories arriving at the Galapagos at 13 km and for all seasons.

Figure 13. Ozone mixing ratio profile at Samoa on October 30, 1998. The thicker solid line is the ozone mixing ratio. The thinner line to the right is the air temperature and the thinner line to the left is the frost-point temperature.

Figure 14. Ten- day back trajectory arriving at Samoa a 5km at 00Z on October 30, 1998. The numbers along the trajectory path mark the number of days back in time the air parcel was located. The elevation change of the air parcel is shown in the lower panel.

Figure 15. Ozone mixing ratio profiles at Samoa on a) October 2, 1997 and

b) October 30, 1997.

Figure 16. Trajectories to Samoa at 5 km on a) October 2, 1997 and b) October 30, 1997.

Figure 17. Ozone mixing ratio profile at Tahiti on October 30, 1998.

Figure 18. Trajectory to Tahiti at 5 km on October 31 1998 at 12Z.

Figure 19. Ozone mixing ratio profile at a) Fiji on November 19, 1997 and b) Samoa on November 20, 1997.

Figure 20. Trajectories to Fiji at 8 km on a) November 20, 1997 and b) November 23, 1997, and to Samoa c) at 6 km on November 20, 1997 and d) at 10 km on November 21, 1997.

Figure 21. Ozone mixing ratio profile at Samoa on February 20, 1999.

Figure 22. Trajectory to Samoa at 6 km on February 21, 1999 at 00Z.

Figure 23. Ozone mixing ratio profile at the Galapagos on October 9, 1999. The thicker solid line is the ozone mixing ratio. The thinner line to the right is the air temperature and the thinner line to the left is the frost-point temperature.

Figure 24. Trajectory to the Galapagos at 6 km on October 9, 1999 at 00Z and 12Z.

Figure 25. Ozone mixing ratio profiles at the Galapagos on a) March 25, 1999 and b) April 4, 1998.

Figure 26. Trajectories to the Galapagos at 6 km on a) March 25, 1999 and b) April 4, 1998.

Ozone in the Pacific Tropical Troposphere From Ozonesonde Observations

S.J. Oltmans[1], B.J. Johnson[1], J.M. Harris[1], H. Vömel[1,2], K. Koshy[3], P. Simon,[4], R. Bendura[5], A.M. Thompson[6], J.A. Logan[7], F. Hasebe[8], M. Shiotani[9], M. Maata[3], G. Sami[3], A. Samad[3], J. Tabuadravu[3], H. Enriquez[10], M. Agama[11], J. Cornejo[11], and F. Paredes[11]

[1] NOAA, Climate Monitoring and Diagnostics Laboratory (CMDL), Boulder, CO 80305, USA

[2] Cooperative Institute for Research in the Environmental Sciences (CIRES), University of Colorado, Boulder, CO, 80309, USA

[3] University of the South Pacific, Suva, Fiji

[4] MeteoFrance, Papeete, Tahiti, French Polynesia

[5] NASA, Langley Research Center, Hampton, VA, USA

[6] NASA, Goddard Space Flight Center, Greenbelt, MD, USA

[7] Harvard University, Cambridge, MA, USA

[8] Ibaraki University, Mito, Japan

[9] Hokkaido University, Sapporo, Japan

[10] INAMHI, Quito, Ecuador

[11] INAMHI, San Cristobal, Galapagos, Ecuador

ABSTRACT: Ozone vertical profile measurements obtained from ozonesondes flown at Fiji, Samoa, Tahiti and the Galapagos are used to characterize ozone in the troposphere over the tropical Pacific. There is a significant seasonal variation at each of these sites. At sites in both the eastern and western Pacific, ozone is highest at almost all levels in the troposphere during the September-November season and lowest during March-May. There is a relative maximum at all of the sites in the mid-troposphere during all seasons of the year (the largest amounts are usually found near the tropopause). This maximum is particularly pronounced during the September-November season. On average, throughout the troposphere at all seasons, the Galapagos has larger ozone amounts than the western

Pacific sites. A trajectory climatology is used to identify the major flow regimes that are associated with the characteristic ozone behavior at various altitudes and seasons. The enhanced ozone seen in the mid-troposphere during September-November is associated with flow from the continents. In the western Pacific this flow is usually from southern Africa (although 10-day trajectories do not always reach the continent), but also may come from Australia and Indonesia. In the Galapagos the ozone peak in the mid-troposphere is seen in flow from the South American continent and particularly from northern Brazil. The time of year and flow characteristics associated with the ozone mixing ratio peaks seen in both the western and eastern Pacific suggest that these enhanced ozone values result from biomass burning. In the upper troposphere low ozone amounts are seen with flow that originates in the convective western Pacific.

Introduction

The tropical Pacific is often considered to be a region remote from major polluting influences because of its isolation from heavily industrialized landmasses. Recent field campaigns (Hoell et al., 1999) have emphasized that though this is often the case, the signature of pollution, particularly from biomass burning, makes a significant imprint on the air chemistry of the region. In a number of instances layers of enhanced ozone (mixing ratios >80 ppbv) were found in the mid-troposphere in the remote western Pacific (Stoller, et al., 1999). These layers in addition to having enhanced ozone were replete with markers of biomass burning (Gregory et al.,1999).

Beginning in August 1995 as part of the Pacific Exploratory Mission (PEM) Tropics A, ozone vertical profile measurements were started at Pago Pago, American Samoa (14.3S, 170.6W) and Papeete, Tahiti (18.0S, 149.0W). At Samoa profiles were also obtained as part of an earlier measurement program from 1986-1989. These earlier profiles provide an opportunity for comparison with measurements during the more recent period. Profile measurements were continued at Tahiti and Samoa through PEM Tropics B with the program at Tahiti completed in December 1999. At Samoa weekly soundings continue as part of the Southern Hemisphere Additional Ozonesondes (SHADOZ) project. During most of the measurement period soundings were done weekly. During the aircraft field campaigns in September-October 1996 (PEM Tropics A) and March-April 1999 (PEM Tropics B) soundings were done twice a week. In January 1997 weekly soundings were begun at Suva, Fiji (18.1S, 178.2E) in anticipation of PEM Tropics B. As part of the Soundings of Ozone and Water Vapor in the Equatorial Region (SOWER) project ozone profile measurements were started on a campaign basis in March 1998 at San Cristobal, Galapgos (0.9S, 89.6W), were increased to bi-weekly soundings in September 1998, and to weekly soundings as part of SHADOZ early in 1999. Soundings continue at Fiji and the Galapagos in 2000 as part of SHADOZ and SOWER.

This set of ozone profiles obtained using balloon-borne ozonesondes provides information on the distribution of ozone throughout the troposphere of the tropical Pacific that has not been available in the past. In particular, new insights on the short-term and seasonal variability of ozone in this region as well as differences between the eastern and western Pacific can be gleaned from these data. In addition, isentropic trajectories are

used to look at the transport associated with particular features of individual profiles, and also at the influence of climatological transport patterns on the principle features of the ozone distribution in the tropical troposphere in this region.

Methods

Ozonesondes

The ozone vertical profiles were obtained using the electrochemical concentration cell (ECC) ozonesonde (Komhyr et al., 1995). This has become a standard technique for obtaining ozone profiles with high vertical resolution in both the troposphere and stratosphere to altitudes of approximately 35 km. The measurements of ozone have an accuracy of ±5% through most of the troposphere with somewhat poorer performance (±10%) for very low mixing ratios (<10 ppbv) encountered occasionally in the tropics. The only important interferent in the measurement technique, which is based on the oxidation reaction of ozone with potassium iodide in solution, is sulfur dioxide that is not encountered at these sites at sufficient concentrations to be of significance. The data were obtained with an altitude resolution of about 50 m but for the analysis performed here were averaged into 250 m layers. Only at Samoa are total column ozone measurements from a collocated Dobson spectrophotometer available for comparison with the integrated total ozone from the ozonesonde. These comparisons give an average ratio of 1.03 ± 0.05 between the Dobson total ozone measurement and the integrated total ozone from the ozonesonde, giving confidence that the ozonesonde measured ozone amounts from all of the sites can be compared with each other. During the course of the measurement program a change was made in early 1998 in the sensing solution recipe (Johnson et al.,

2000) at all of the sites except the Galapagos where the new recipe was used from the beginning. This change primarily affects the measurements in the stratosphere. From comparison flights made at these sites, as well as laboratory tests, an empirical correction has been derived, and the earlier data have been corrected using this relationship. Data archived in the Global Troposhere Experiment (GTE) archive for PEM Tropics at NASA Langley have this correction applied.

Trajectories

For the purposes of characterizing the tropospheric air-flow patterns influencing transport to the tropical sites, insentropic trajectories have been calculated. The trajectories are computed from the ECMWF analyses using the model described in Harris and Kahl (1994). The limitations in such trajectories must be recognized in interpreting the results that are obtained, but they do provide a useful tool for obtaining a picture of the flow patterns that may influence ozone behavior at these sites. The computed trajectories are used both to investigate individual cases, and by grouping the trajectories using an objective clustering technique (Moody, 1986; Harris and Kahl, 1990) that gives an indication of the primary flow regimes influencing a particular location at a given altitude. The trajectories are computed twice daily (00 and 12 UT) for 10 days backward in time. Air parcels reaching a site after 10 days of travel may have undergone diabatic processes that are not accounted for in the model used here, and these are an important contribution to the uncertainty in the computed pathway of the air parcel (Merrill, 1996). Transport from sources or sinks more than 10 days travel time from a particular site could also have a significant influence on ozone levels measured at the site.

Day-to-day variations

Variations on the order of several days are a large source of the variability seen in tropospheric ozone at the Pacific tropical sites studied here as will be shown in the analysis in this section. These variations have been studied from surface observations at Samoa (Harris and Oltmans, 1998). The surface variations were found to result from changes in airflow to the site that tapped different sources and sinks. During all seasons air coming from higher latitudes and altitudes has about 50% more ozone than air with a tropical origin (Harris and Oltmans, 1998). Although the ozone soundings are done on an approximately weekly schedule compared to the continuous observations at the surface, the variability from sounding-to-sounding captured in the time-height cross-section of ozone mixing ratio for 1996 at Samoa (Plate 1) is also apparent. During 1996 at Samoa the soundings were done twice a week during September and October so that the variability is well represented during this time of the year. This can also be seen in the plot of the average profiles at 0.25 km increments for individual seasons at Tahiti (Figure 1). The median is the horizontal line inside of the box, and the box represents the inner 50^{th} percentile of the data. The whiskers represent the inner 90^{th} percentile of the data. The solid diamond is the mean. The September-November period has greatly enhanced variability especially in the 2-10km layer when compared to the March-May period. These seasonal profiles are based on several years of data, and represent the variability that is primarily contributed by the short-term fluctuations within a season.

In the Galapagos the time-height cross-section for 1999 (Plate 2), the only complete year available for this site, shows many of the same features seen at Samoa. The seasonal profiles for the Galapagos (figure 2) show similar behavior to Tahiti with a maximum in the variability in September-November and a minimum in the March-May season. The variability is greater at Tahiti in September-November than it is in the Galapagos. At Samoa (Figure 3) the variability in this season is also larger than at the Galapagos but not quite as large as at Tahiti. Since Fiji (Figure 4) also shows greater variability during this season, the larger variability is likely a real difference between the eastern and western Pacific.

Seasonal variation

As can be seen in figures 1 - 4, not only is the variability of ozone in the troposphere greater in September-November than in March-May, but also the mean (and the median) values are greater as well. Time-height cross-sections based on 14-day averages over the entire record of measurements (which varies somewhat for each site) are shown in plate 3. Although there are unique features at each site, a pattern is discernable that is reflected at all sites. In the western Pacific there is a prominent layer of enhanced ozone in the mid-troposphere in September and October. There also seems to be a distinct pulse in June and July of somewhat smaller magnitude with a relative minimum in late July and August. Associated with this June-July enhancement in the mid-troposphere, ozone in the boundary layer also increases and this produces a seasonal maximum near the surface that occurs earlier than the peak in the mid-troposphere. During austral winter and spring higher ozone amounts descend to about 10-12 km giving higher ozone in the upper

troposphere. This seems to be associated with ozone in the lower stratosphere. In January-May ozone at all latitudes is almost always lower than at a corresponding altitude during the rest of the year. Also at this time of year ozone in the upper troposphere is often very low with amounts approaching those seen at the surface which are almost always quite low (<15 ppbv) in this season.

An earlier set of profiles obtained at Samoa from August 1986 – January 1990 (Figure 5) show similar characteristics to those seen in the more recent 5-year data set. For March-May the earlier period has somewhat more ozone that appears to be driven by several profiles with greater ozone amounts, particularly in the low and mid-troposphere (Figure 5a). In September-November, however, the amounts and variability are very similar (Figure 5b).

In the Galapagos the general picture is similar to the western Pacific sites, but with some important differences (Figure 6). The mid-tropospheric ozone maximum occurs earlier in the year and diminishes earlier as well. Near the surface the seasonal variation is smaller. The most noticeable difference is the lack of very low mixing ratios in the middle and upper troposphere especially during the January-May time of year. This is consistent with the fact that the western Pacific is a more convective region where boundary layer air can be mixed into the upper troposphere. Other than this noticeable lack of low ozone amounts the differences among the western Pacific sites is similar to the difference between the eastern and western Pacific. It is also clear that in the Galapagos ozone

amounts are greater than in the western Pacific above 4 km in September-November and above 5 km in March-May .

Flow characteristics

Although the seasonal ozone behavior at all of the sites has some features in common such as the maximum during the austral spring (September-November), this does not by itself imply that the sources and sinks influencing the measured ozone at the sites are the same. For example the proximity of the Galapagos to the South American continent suggests that this continent is more likely to have a greater influence on this site than the western Pacific. The following analysis shows that while the airflow patterns at the western Pacific sites are quite similar, they are much different from those in the Galapagos. The differences in airflow direction with season are greatest in the boundary layer and somewhat greater at all levels in the Galapagos than in the western Pacific. To carry out this analysis a 10-year climatology of 10-day back trajectories was computed at three levels (1, 6, and 13 km) for all four of the sites for each of four seasons. These trajectories were grouped into six clusters at each site for each altitude. Examples representative of various regimes are discussed here (Figures 7-12).

Because of the similarity in flow patterns at the western Pacific sites the description of the behavior at Tahiti is used to indicate the overall pattern with some differences from the other sites noted. At 1 km, a level in the marine boundary layer, the largest seasonal contrast is between December-February (Figure 7a) and June-August (Figure 7b). These are the seasons of minimum and maximum surface ozone at Samoa (Harris and Oltmans,

1997). During the austral summer (Dec.-Feb.) flow at this level is predominantly from the tropical Pacific for all of the sites in the western Pacific. In the other seasons 15-65% of the flow is from the west and more southerly latitudes with the largest percentage of flow from the south occurring in austral winter. Fiji shows this most prominently with 65% of the trajectories coming from the south and west during June-August while at Tahiti and Samoa the percentage of southerly flow is closer to 30% (Figure 7b).

At 6 km at Tahiti flow (Figure 8) is more uniformly from the west with only about 20% coming from the east on an annual basis. There is a southerly component to the airflow but it usually does not extend south of 40S within 10 days, in contrast to the low level flow that reaches much higher latitudes. Throughout the austral winter and spring (June-November) at least 25% of the trajectories arriving at Tahiti come from as far west as the mid Indian Ocean and about 10% reach southern Africa (Figure 8b) within 10 days. To Fiji the flow is even more vigorous from the west and about 5% of the trajectories come from South America. A number of trajectories also have their 10-day origins over northern Australia. In the summer flow is less vigorous and some trajectories have a northerly component.

In the upper troposphere (13 km) the flow is from the west but a majority of the trajectories also have a northerly component (Figure 9). This northerly flow brings air from near or even north of the equator and is strongest in September-November but is present in other seasons as well. As in the mid-troposphere, a significant number of the trajectories come from the Indian Ocean and Africa.

The flow patterns in the Galapagos differ significantly from those in the western Pacific. At the lowest level (Figure 10) the flow is overwhelmingly from the south and over the ocean in all seasons. There is some variation with season with December-May showing 10-15% of the trajectories coming from the Atlantic. In June-November the flow is exclusively from the south, often paralleling the South American coast. The flow at 6 km is in strong contrast to that in the boundary layer. On an annual basis 75% of the trajectories arrive at San Cristobal from the east and have passed over the South American continent in the previous 10 days. In December-February (Figure 11a) about 10% of trajectories arrive from the tropical north Pacific, another 10% from the tropical south Pacific, and the remainder from the east off continental South America. During June-November (June-August shown in Figure 11b) about 10-15% of the flow is from the tropical south Pacific with the remainder from the east or with little movement (cluster 3 in figure 11b). At 13 km (Figure 12) the flow is about equally divided into weak flow from the east or northeast and vigorous flow from the west. There is a fairly strong seasonality with December-May dominated by trajectories arriving from the west, but about half the trajectories during June-November come from the east and northeast.

Discussion

In the previous sections the day-to-day and seasonal variations have been described as well as the major air flow characteristics affecting the ozonesonde sites in the western and eastern tropical Pacific. In this section important features of the ozone profile are linked to the trajectories to show how important source and sink regions for ozone may

contribute to both the shorter term and seasonal variations. Since the tropics are known to be a significant area of biomass burning (see TRACE-A and SAFARI Special Issue of the *Journal of Geophysical Research, 101*, 1996) particular attention is paid to characterizing the possible influence of burning on ozone at these sites by linking enhanced ozone layers with flow from potential source regions. It appears that several burning regions contribute to what is seen at these sites. The low ozone mixing ratios seen in the upper troposphere at the western Pacific sites are also briefly discussed.

It is clearly seen from Plate 3 that there is a persistent layer of enhanced ozone in the mid-troposphere in the June-November season. The climitological trajectory analysis also shows this season to be one of regular occurrences of flow from potential burning related source regions in southern Africa and Australia for the western locations and South America for San Cristobal. Several individual profiles are examined that contain enhanced mid-tropospheric ozone along with the trajectories calculated for these cases. Profiles that show little or no ozone enhancement are also examined in relation to flow characteristics. An event of very high ozone seen at Fiji and Samoa in November 1997 is investigated because the flow path suggests an Indonesian source for the enhanced ozone.

A profile with an enhanced mid-tropospheric layer characteristic of those seen during the September and October period in the western Pacific is shown in figure 13 for a sounding done at Samoa on October 30, 1998. The peak ozone mixing ratio of 105 ppbv at ~6 km has a trajectory (Figure 14) that reaches back to southern Africa 10 days prior to the sounding. Ozone profiles with peaks greater than about 70 ppbv (Figure 15) do not

In 1997 extensive burning took place in Indonesia associated with drought conditions that were a consequence of the strong El Nino. Ozone profile measurements over the Indonesian region have shown high ozone was found in Indonesia and Malaysia in connection with the burning in the region (Fujiwara et al., 1999). On November 19 and 20 at Fiji and Samoa (Figures 19) some of the highest tropospheric ozone amounts were seen for any event recorded at these sites. These enhancements, which encompassed the entire troposphere above the two sites, increased the total tropospheric column by about 20 DU, or more than 70% over average values for the month. The trajectories show that at both sites air was coming from Indonesia (Figure 20a-d) throughout the depth of the tropospheric column. Although these profiles were the only ones measured during the event, trajectories show that a flow pattern nearly identical with the one during this large ozone enhancement persisted for about 5 days around the time that the profiles were obtained (Figure 20d).

As was noted earlier, during the austral summer ozone is generally quite low throughout the troposphere in the western Pacific. Low values less than 10 ppbv are seen as in the profile for February 20, 1999 at Samoa (Figure 21) where in the 13-15 km layer ozone is about 5 ppbv. The trajectory at 13 km (Figure 22) shows that air came from northeast of Australia in a region associated with extensive convection during this time of year. The low ozone mixing ratios are not usually a result of mixing directly from the surface near the site, although surface mixing ratios are low enough. This can be seen in Plate 3a, 3c, and 3d where the minima in the upper troposphere are not connected to the low values at the surface as illustrated by the individual profile shown in figure 21. Instead there is

normally a relative maximum in the mixing ratio in the mid-troposphere. It is more likely that air with very low ozone is mixed vertically by convection in the region of northern Australia and eastern Indonesia and transported to these sites in the upper troposphere (Kley et al., 1997).

In the Galapagos many of the profiles during August-October also show pronounced mid-tropospheric peaks (Figure 23) as seen on October 9, 1999. The trajectory for this event (Figure 24) crosses Brazil in less than 10 days over a region that is heavily influenced by biomass burning during this time of the year (Fishman et al., 1996). Investigation of each profile with an enhanced ozone layer in the mid-troposphere during this time of the year showed a trajectory that passed over Brazil. At times of the year when burning is not happening in Brazil, profiles at the Galapagos do not show pronounced tropospheric peaks (Figure 25). Profiles with mixing ratios near 50 ppbv in the mid-troposphere are occasionally seen (Figure 25a). These higher amounts are generally associated with flow from continental South America (Figure 26a). However, flow from the continent may also have relatively low ozone amounts (Figures 25b and 26b). It appears that even though transport to the site is similar, that unless this flow taps a source region with higher ozone, that passing over a continent is not sufficient (although it does appear necessary) to give enhancements in the ozone amount. This was also near the end of the 1997-98 ENSO warm phase with well above normal precipitation both in the Galapagos and western equatorial South America. The profile of April 4 suggests that convection has influenced the profile since humidity is high up to about 9 km (the depression between the air temperature and frost-point temperature shown in figure 22b is small).

Conclusions

From an extensive set of ozone profiles obtained over the past several years in the tropical Pacific, a picture emerges of a region of both very low tropospheric ozone amounts (~10 ppbv) and surprisingly large (~100 ppbv) concentrations that are found at all of the sites studied. The low concentrations are expected in light of the strong photochemical sink in this region (Kley, et al., 1997), and the important role of convection, particularly during the austral summer. On the other hand the ubiquitous presence of mid-tropospheric layers of enhanced ozone demonstrates that the influence of biomass burning is widespread throughout the tropical zone during August-November. On average ozone at the equatorial Galapagos site in the eastern Pacific is greater than at the three western tropical Pacific sites. However, for individual profiles, the mid-tropospheric enhancements seen in the western Pacific attain larger mixing ratios than seen in the Galapagos. This is in spite of the fact that the Galapagos are located much closer to the potential source of burning-produced ozone in Brazil than the western Pacific sites are to the south African burning sources. The relative proximity of sources in Australia and Indonesia may, however, partially account for this. Alternatively, the much greater amount of biomass burned in southern Africa may produce larger ozone enhancements (Olson et al., 1999). The extensive burning that took place in Indonesia during the latter half of 1997 appears to have been the source of very large ozone amounts seen in Samoa and Fiji in November 1997.

References:

Fishman, J., J.M. Hoell Jr., R.D. Bendura, R.J. McNeal, V.W.J.H. Kirchhoff, NASA GTE TRACE A Experiment (September-October 1992): Overview, *J. Geophys. Res., 101*, 23,865-23,879, 1996.

Fujiwara, M., K. Kita, S. Kawakami, T. Ogawa, N. Komala, S. Saraspriya, and A. Suripto, Tropospheric ozone enhancements during the Indonesian forest fire events in 1994 and 1997 as revealed by ground-based observations, *Geophys. Res. Lett., 26*, 2417-2420, 1999.

Gregory, G.L., D.J. Westberg, M.C. Shipham, D.R. Blake, R.E. Newell, H.E. Fuelberg, R.W. Talbot, B.G. Heikes, E.L. Atlas, G.W. Sachse, B.A. Anderson, and D. C. Thornton, Chemical characteristics of Pacific tropospheric air in the region of the Intertropical Convergence Zone and South Pacific Convergence Zone, *J. Geophys. Res., 104*, 6577-5696, 1999.

Harris, J.M, and J.D. Kahl, A descriptive atmospheric transport climatology for the Mauna Loa Observatory, using clustered trajectories, *J. Geophys. Res., 99*, 13,651-13-667, 1990.

Harris, J.M. and J.D. Kahl, Analysis of 10-day isentropic flow patterns for Barrow, Alaska: 1985-1992, *J. Geophys. Res., 99*, 25,845-25855, 1994.

Harris, J.M. and S.J. Oltmans, Variations in tropospheric ozone related to transport at American Samoa, *J. Geophys. Res., 102*, 8781-8791, 1998.

Hoell, J.M, D.D. Davis, D.J. Jacob, M.O. Rogers, R.E. Newell, H.E. Fuelberg, R.J. McNeal, J.L. Raper, and R.J. Bendura, Pacific Exploratory Mission in the tropical Pacific: PEM-Tropics A, August-September 1996, *J. Geophys. Res., 104*, 5567-5583, 1999.

Johnson, B.J., S.J. Oltmans, H. Vömel, and T. Deshler, Characterization of the ECC ozonesonde, *J. Geophys. Res.*, in preparation, 2000.

Kley, D., H.G.J. Smit, H. Vömel, H. Grassl, V. Ramanathan, P.J Crutzen, S. Williams, J. Meywerk and S.J. Oltmans, Tropospheric water-vapour and ozone cross-sections in a zonal plane over the central equatorial Pacific, Q. J. R. Meteor. Soc., 123, 2009-2040, 1997.

Komhyr, W.D., R.A. Barnes, G.B. Brothers, J.A. Lathrop, and D.P. Opperman, Electrochemical concentration cell ozonesonde performance evaluation during STOIC 1989, *J. Geophys. Res., 100*, 9231-9244, 1995.

Merrill, J.T., Trajectory results and interpretation for PEM-West A, *J. Geophys. Res., 101*, 1679-1690, 1996.

Moody, J. L., *The Influence of Meteorology on Precipitation Chemistry at Selected Sites in the Eastern United States,* Ph. D. Thesis, 176pp, University of Michigan, Ann Arbor, Michigan, 1986.

Olson, J.R., B.A. Baum, D.R. Cahoon, J.H. Crawford, Frequency and distribution of forest, savanna and crop fires over tropical regions during PEM Tropics A, *J. Geophys. Res., 104*, 5865-5876, 1999.

Stoller, P., J.Y.N. Cho, R.E. Newell, V. Thomas, Y. Zhu, M.A. Carroll, G.M. Albercook, B.E. Anderson, J.D.W. Barrick, E.V. Browell, G.L. Gregory, G.W. Sachse, S. Vay, J.D. Bradshaw, and S. Sandholm, Measurement of atmospheric layers from the NASA DC-8 and P3-B aircraft during PEM-Tropics A, *J. Geophys. Res., 104*, 5745-5764, 1999.

Plate Captions:

Plate 1. Time-height cross-section of ozone mixing ratio at Pago Pago, American Samoa for 1996. Soundings are weekly except during the PEM Tropics A intensive measurement period from August-September when soundings were done twice weekly

Plate 2. Time-height cross-section of ozone mixing ratio from weekly soundings at San Cristobal, Galapagos for 1999.

Plate 3. Time-height cross-sections of ozone mixing ratio based on 14-day averages over the entire record of measurements at Samoa, Galapagos, Fiji, and Tahiti.

Figure Captions:

Figure 1. The average ozone profile and variability for 0.25 km layers at Tahiti for two seasons (March-May and September-November) for the period 1995-1999. The median is the horizontal line inside the box, and the box represents the inner 50^{th} percentile of the data. The "whiskers" represent the inner 90^{th} percentile of the data. The solid diamond is the mean.

Figure 2. Average ozone profile and variability for 0.25 km layers at Galapagos for two seasons (March-May and September-November) for the period 1998-2000.

Figure 3. Average ozone profile and variability for 0.25 km layers at Samoa for two seasons (March-May and September-November) for the period 1995-2000.

Figure 4. Average ozone profile and variability for 0.25 km layers at Fiji for two seasons (March-May and September-November) for the period 1997-2000.

Figure 5. Comparison of ozone mixing ratio profiles at Samoa from two time periods; 1986-1989 and 1995-2000 for a) March-May and b) September-November.

Figure 6. Comparison of the ozone mixing ratio profiles at Samoa and the Galapagos for March-May and September-November.

Figure 7. Clusters of trajectories arriving at Tahiti at 1 km for a) December-February and b) September-November for the period 1990-1999. The clusters are numbered 1-6 and the percentage of the total number of trajectories in each cluster is also shown.

Figure 8. Clusters of trajectories arriving at Tahiti at 6 km and for a) March-May and b) September-November.

Figure 9. Clusters of trajectories arriving at Tahiti at 13 km and for all seasons.

Figure 10. Clusters of trajectories arriving at the Galapagos at 1 km and for all seasons.

Figure 11. Clusters of trajectories arriving at the Galapagos at 6 km and for a) December –February and b) June-August.

Figure 12. Clusters of trajectories arriving at the Galapagos at 13 km and for all seasons.

Figure 13. Ozone mixing ratio profile at Samoa on October 30, 1998. The thicker solid line is the ozone mixing ratio. The thinner line to the right is the air temperature and the thinner line to the left is the frost-point temperature.

Figure 14. Ten- day back trajectory arriving at Samoa a 5km at 00Z on October 30, 1998. The numbers along the trajectory path mark the number of days back in time the air parcel was located. The elevation change of the air parcel is shown in the lower panel.

Figure 15. Ozone mixing ratio profiles at Samoa on a) October 2, 1997 and

b) October 30, 1997.

Figure 16. Trajectories to Samoa at 5 km on a) October 2, 1997 and b) October 30, 1997.

Figure 17. Ozone mixing ratio profile at Tahiti on October 30, 1998.

Figure 18. Trajectory to Tahiti at 5 km on October 31 1998 at 12Z.

Figure 19. Ozone mixing ratio profile at a) Fiji on November 19, 1997 and b) Samoa on November 20, 1997.

Figure 20. Trajectories to Fiji at 8 km on a) November 20, 1997 and b) November 23, 1997, and to Samoa c) at 6 km on November 20, 1997 and d) at 10 km on November 21, 1997.

Figure 21. Ozone mixing ratio profile at Samoa on February 20, 1999.

Figure 22. Trajectory to Samoa at 6 km on February 21, 1999 at 00Z.

Figure 23. Ozone mixing ratio profile at the Galapagos on October 9, 1999. The thicker solid line is the ozone mixing ratio. The thinner line to the right is the air temperature and the thinner line to the left is the frost-point temperature.

Figure 24. Trajectory to the Galapagos at 6 km on October 9, 1999 at 00Z and 12Z.

Figure 25. Ozone mixing ratio profiles at the Galapagos on a) March 25, 1999 and b) April 4, 1998.

Figure 26. Trajectories to the Galapagos at 6 km on a) March 25, 1999 and b) April 4, 1998.

Plate 2. Time-height cross-section of ozone mixing ratio from weekly soundings at San Cristobal, Galapagos for 1999.

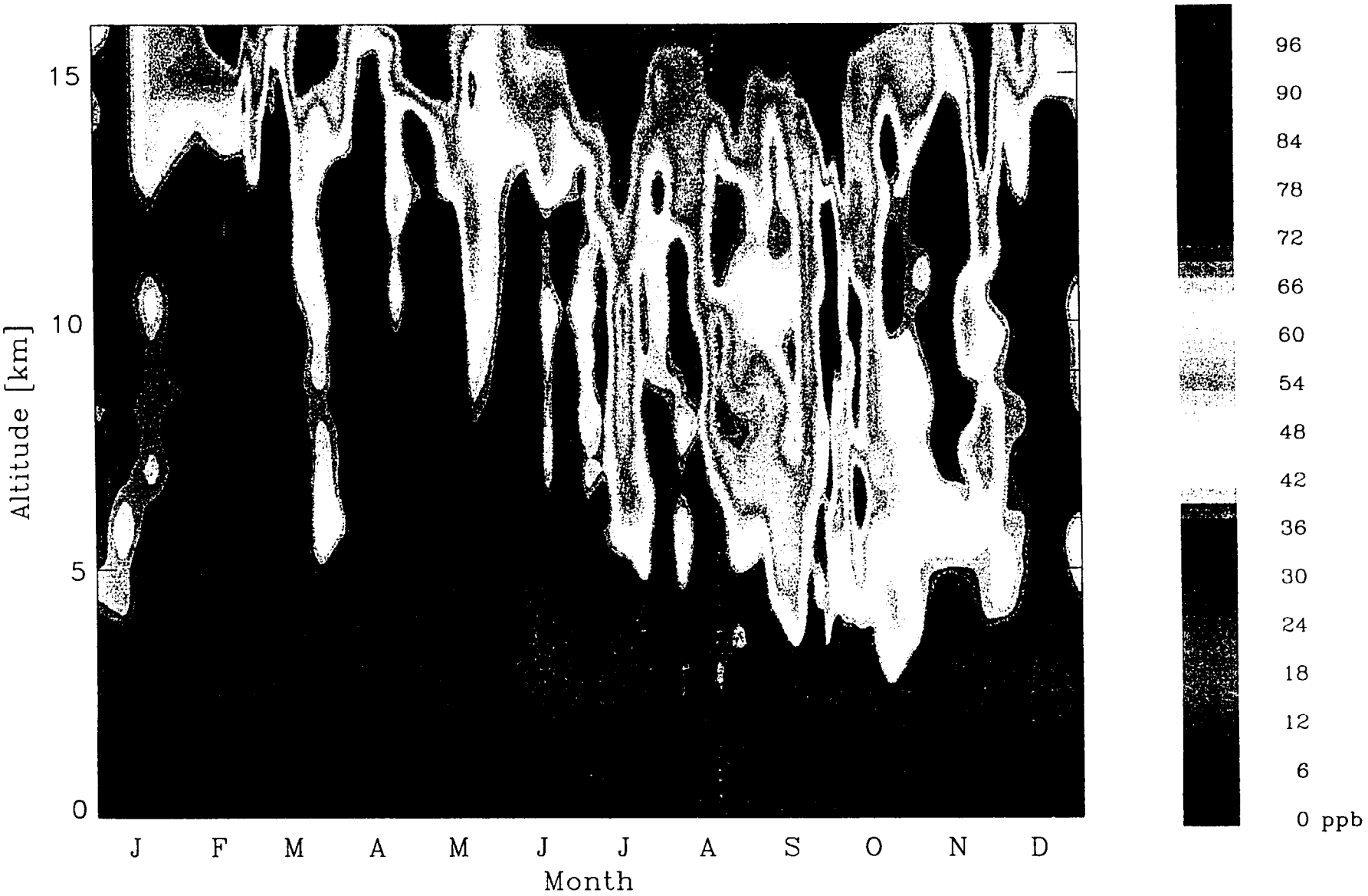

Plate 3. Time-height cross-sections of ozone mixing ratio based on 14-day averages over the entire record of measurements at Samoa, Galapagos, Fiji, and Tahiti.

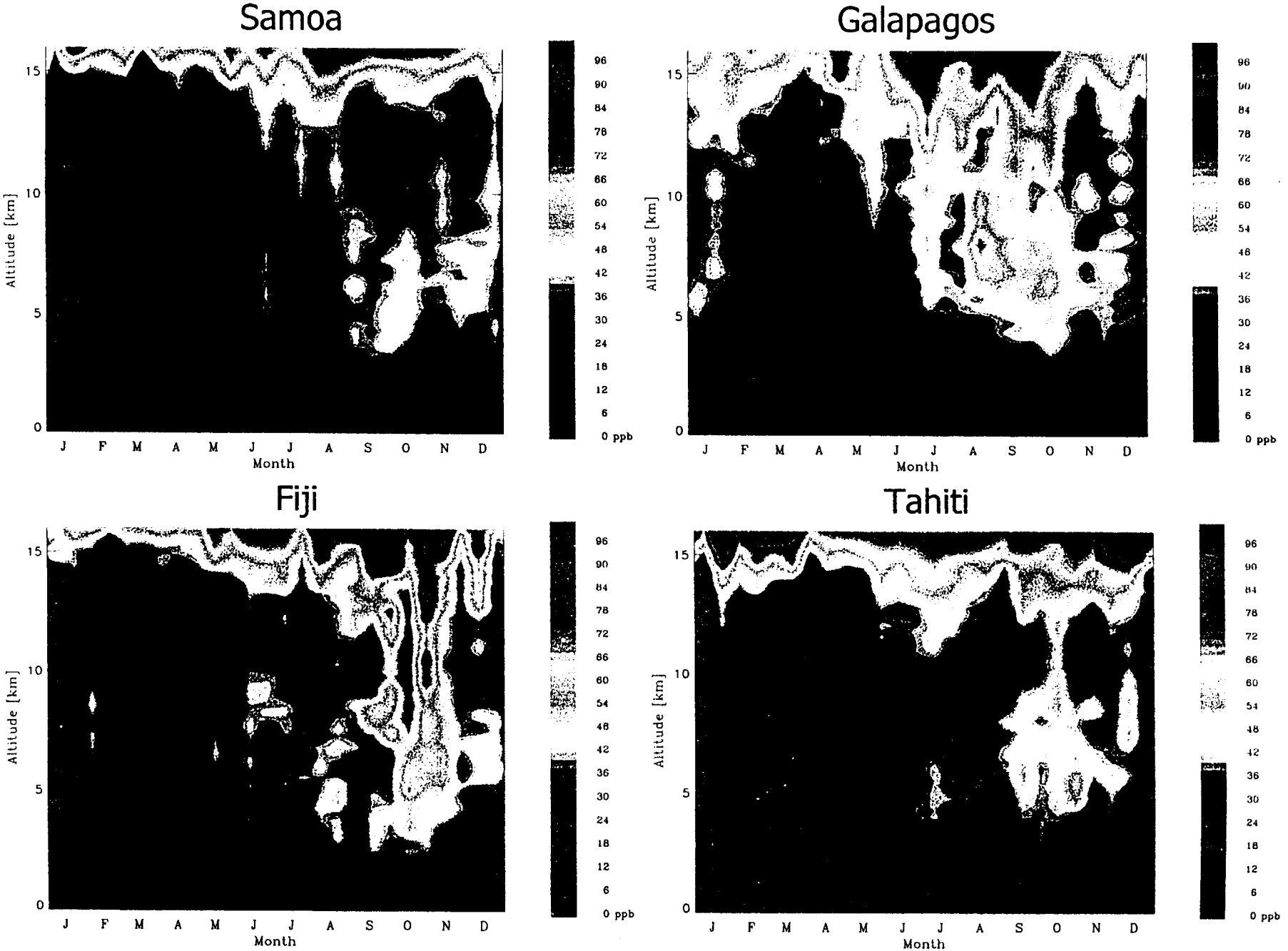

Figure 1. Average ozone profile and variability for 0.25 km layers at Tahiti for two seasons (March-May and September-November) for the period 1995-1999. The median is the horizontal line inside the box, and the box represents the inner 50th percentile of the data. The "whiskers" represent the inner 90th percentile of the data. The solid diamond is the mean.

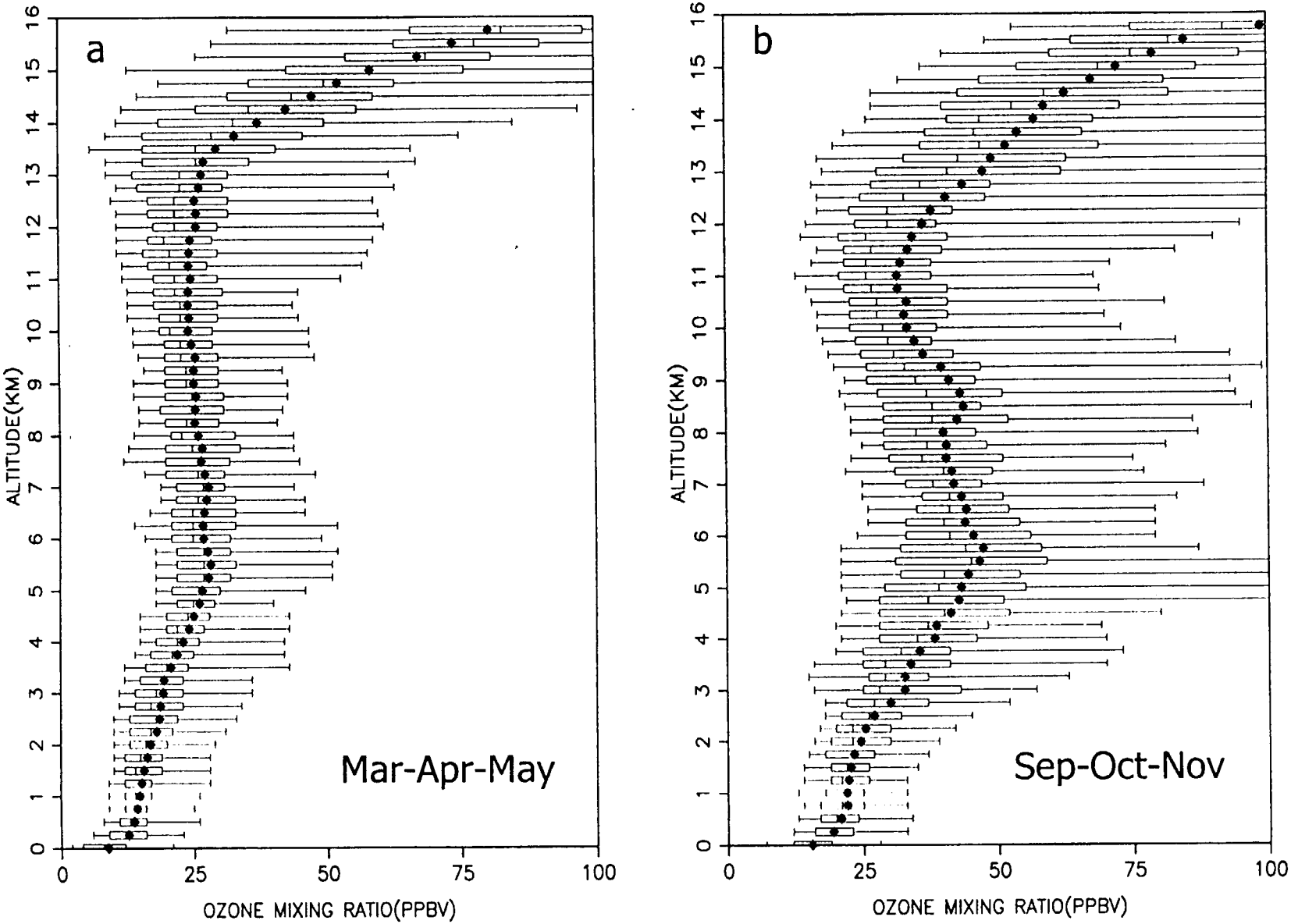

Figure 2. Average ozone profile and variability for 0.25 km layers at Galapagos for two seasons (March-May and September-November) for the period 1998-2000.

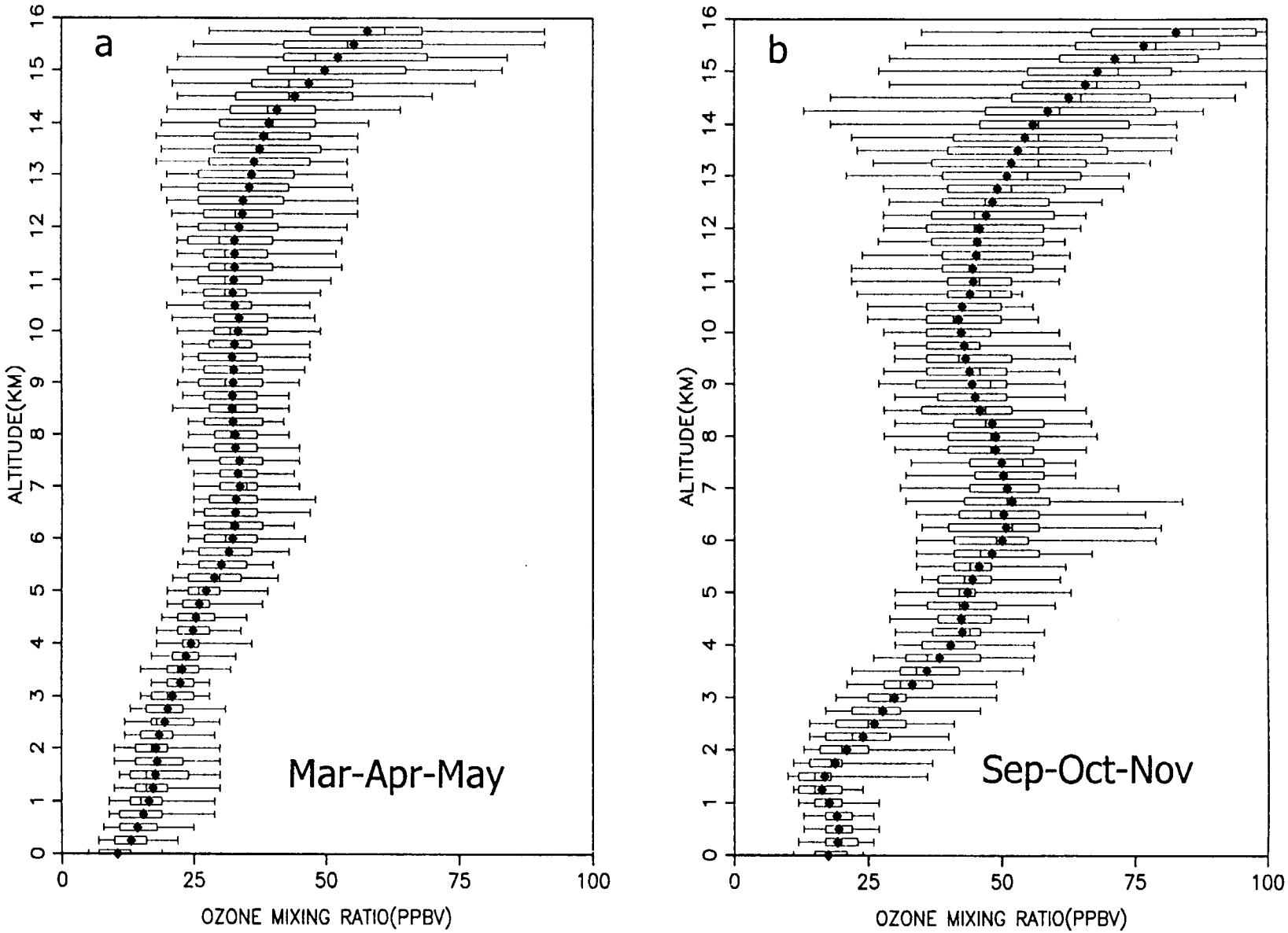

Figure 3. Average ozone profile and variability for 0.25 km layers at Samoa for two seasons (March-May and September-November).

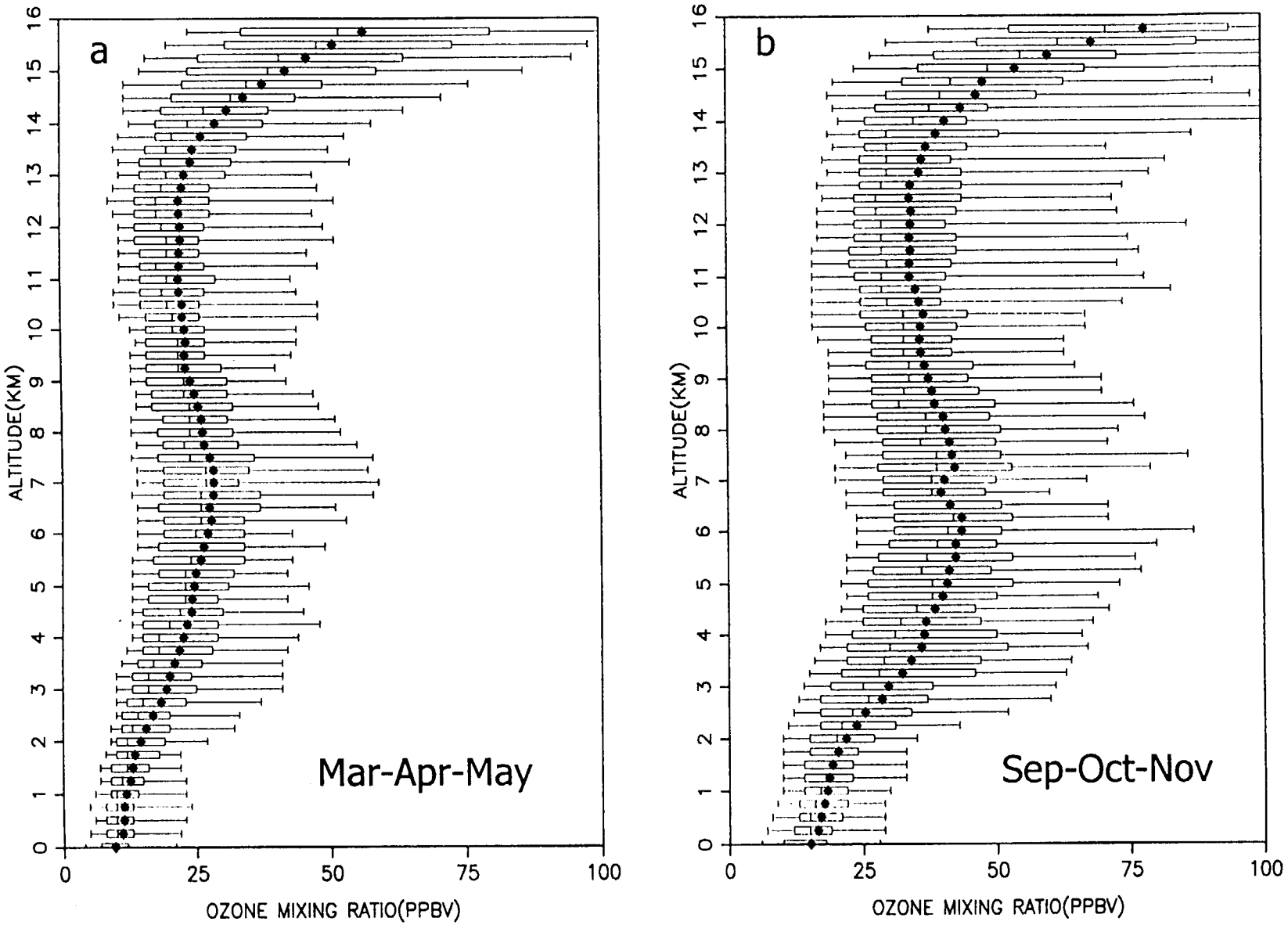

Figure 4. Average ozone profile and variability for 0.25 km layers at Fiji for two seasons (March-May and September-November).

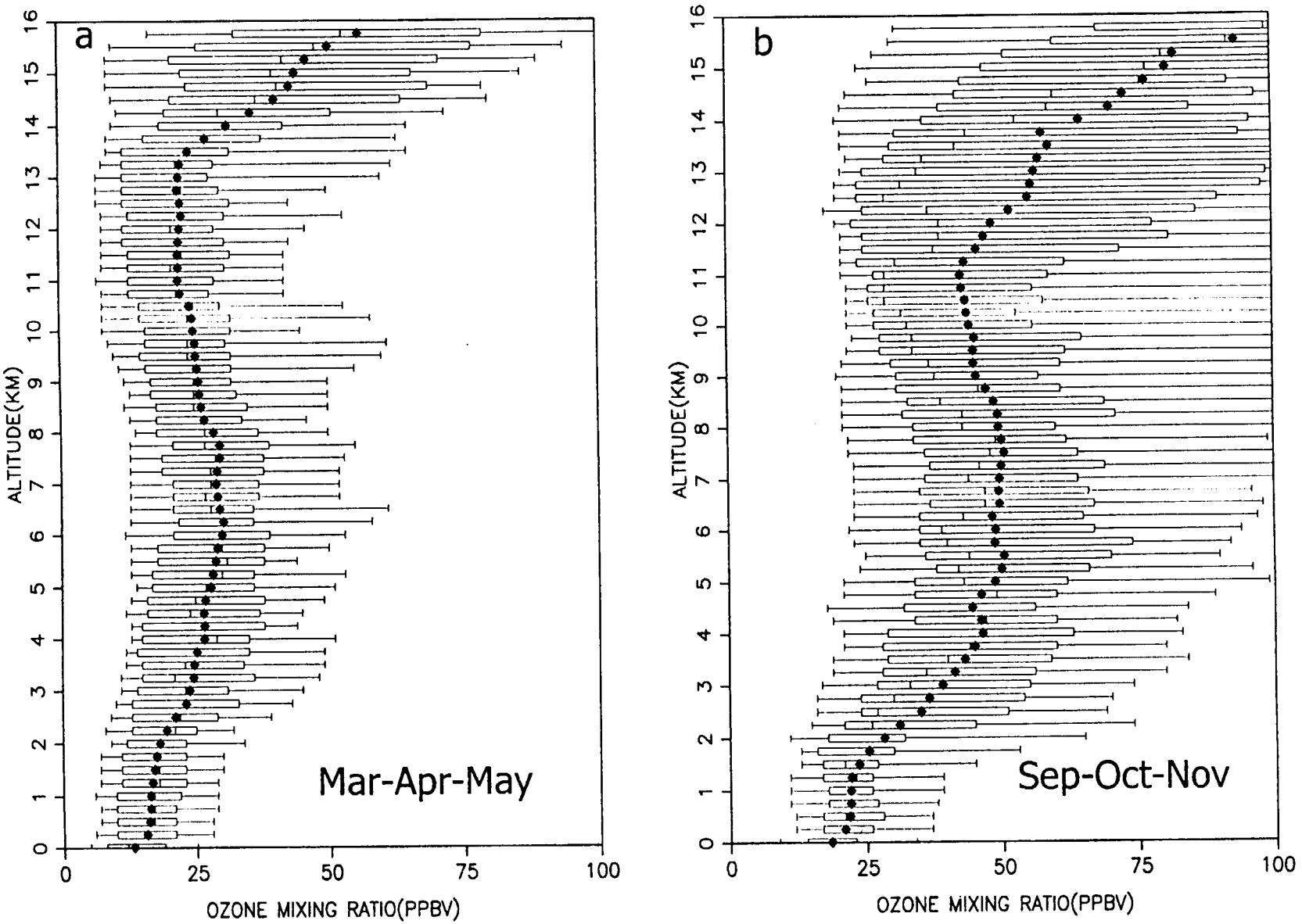

Figure 5. Comparison of the ozone mixing ratio profiles at Samoa for the periods 1986-1989 and 1995-2000 for a) March-May and b) September-November.

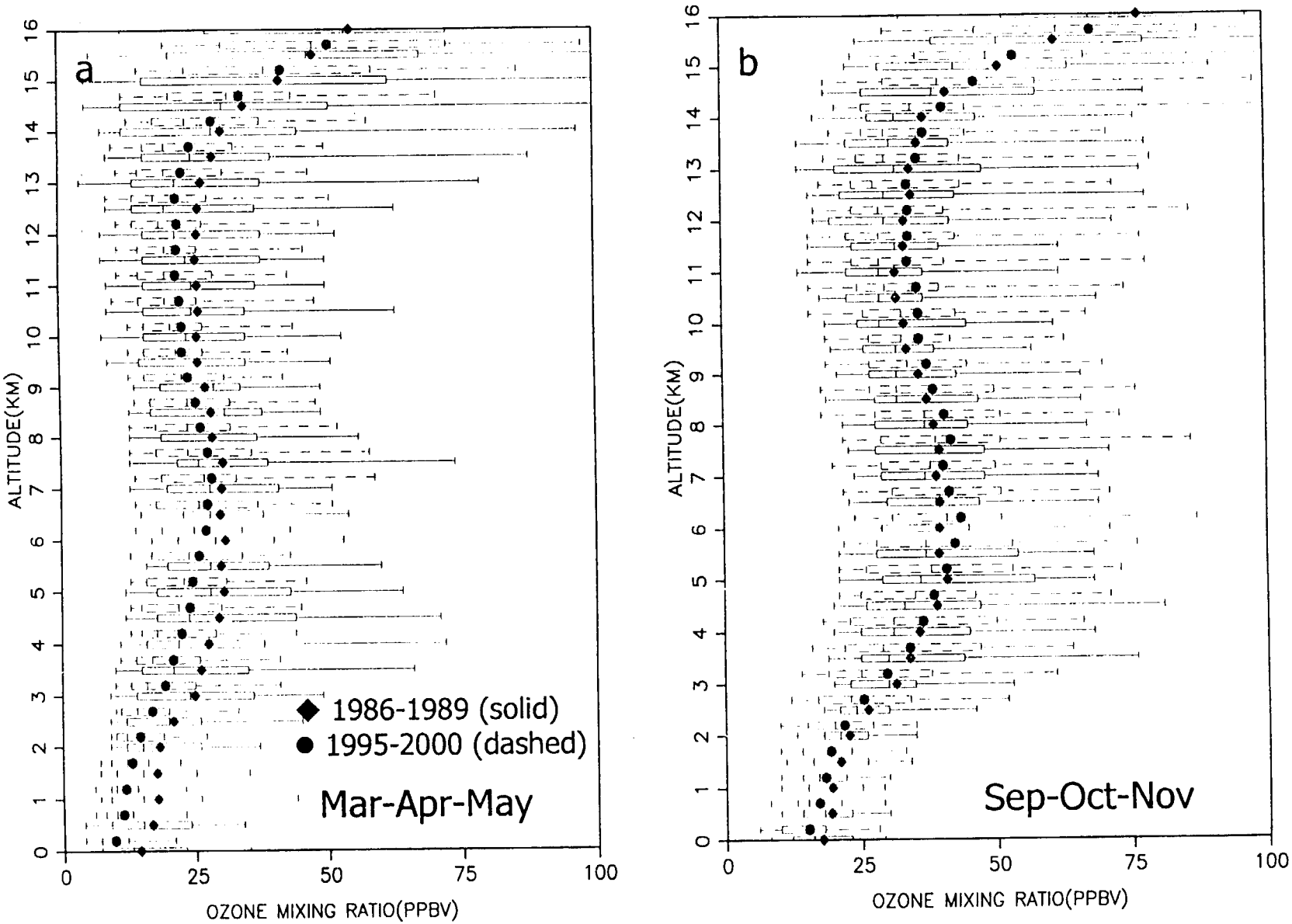

Figure 6. Comparison of the ozone mixing ratio profiles at Samoa and the Galapagos for a) March-May and b) September-November.

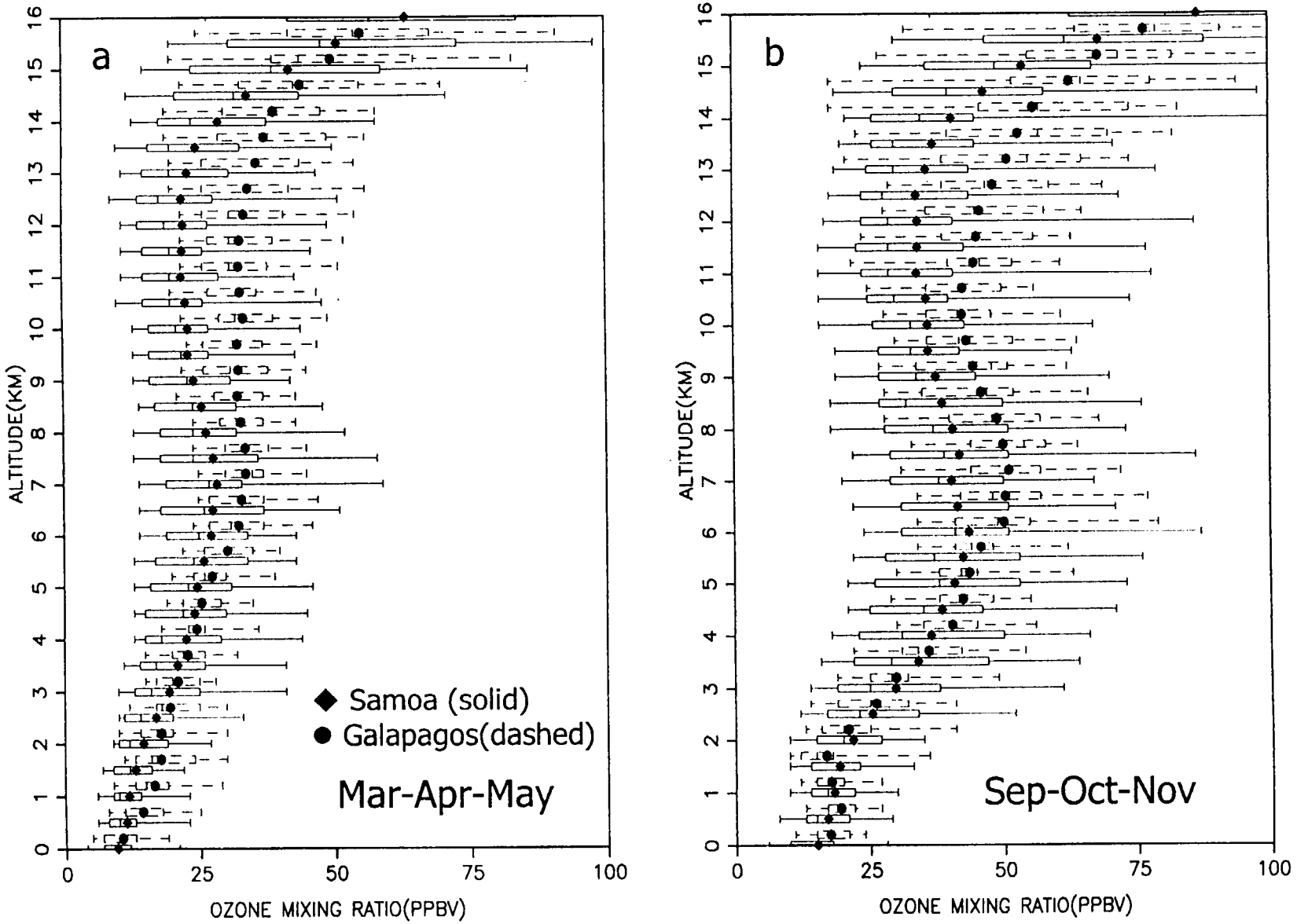

Figure 7a. Clusters of trajectories arriving at Tahiti at 1 km for December-February for the period 1990-1999. The clusters are numbered 1-6 and the percentage of the total number of trajectories in each cluster is also shown.

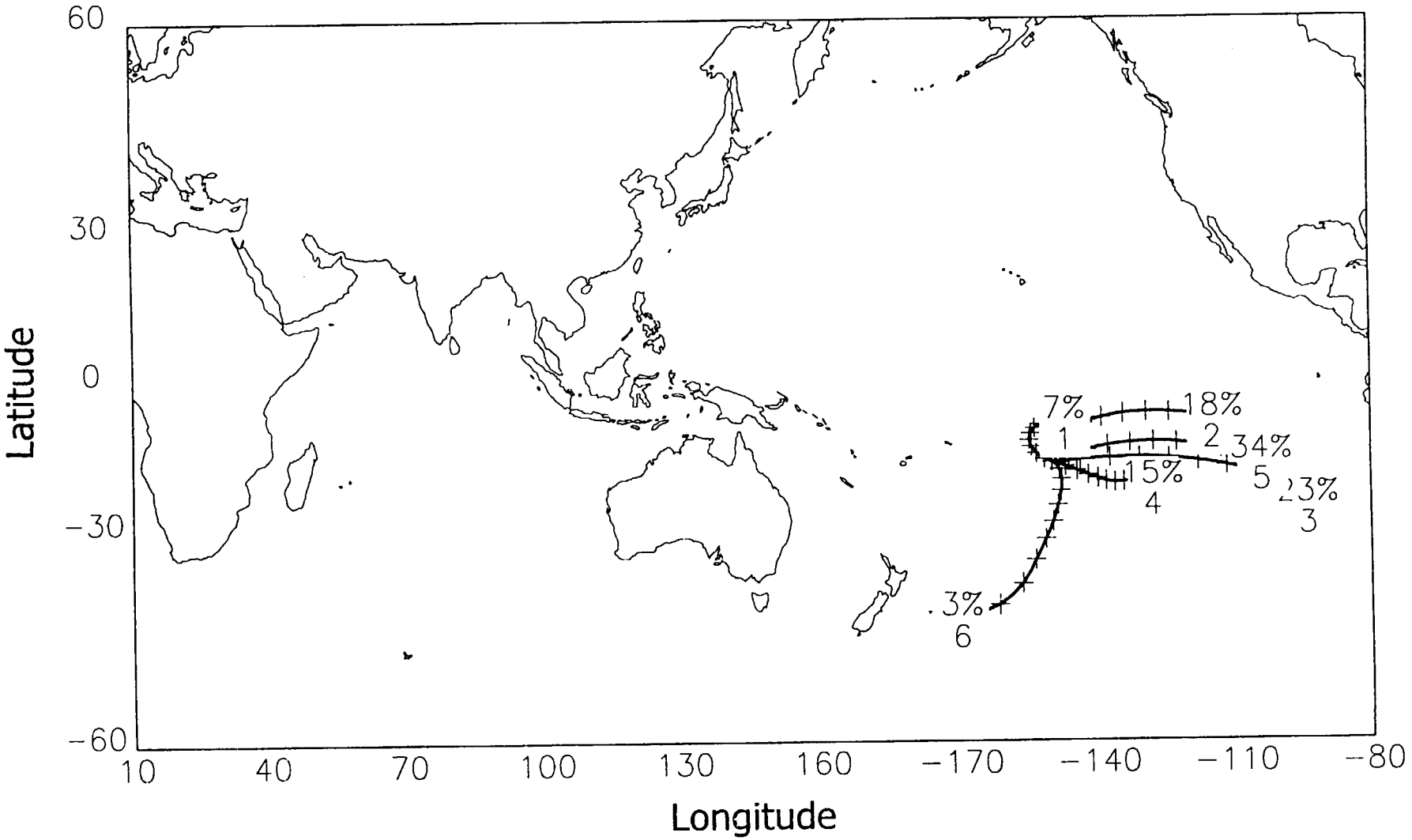

Figure 7b. Clusters of trajectories arriving at Tahiti at 1 km for September-November for the period 1990-1999. The clusters are numbered 1-6 and the percentage of the total number of trajectories in each cluster is also shown.

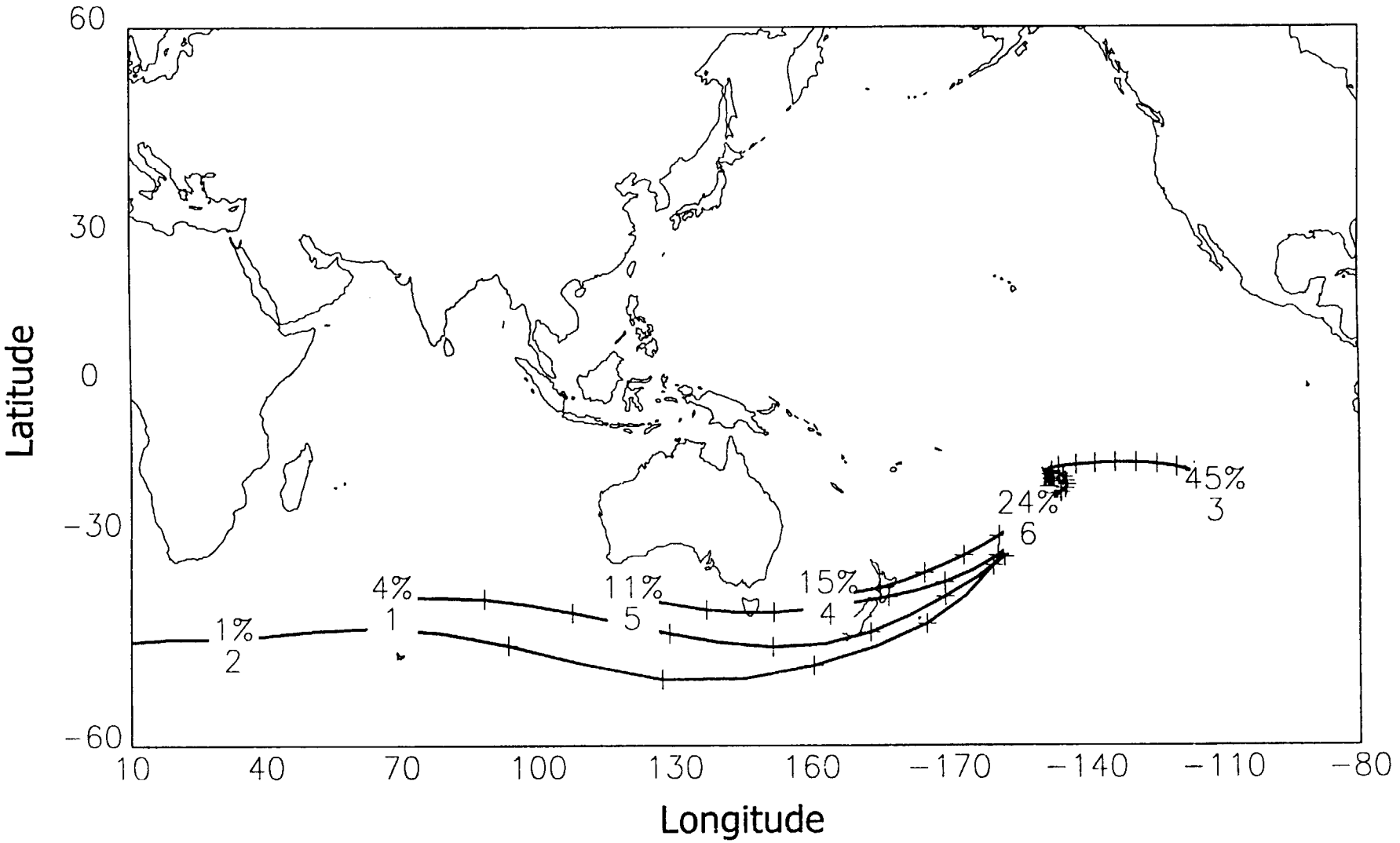

Figure 8a. Clusters of trajectories arriving at Tahiti at 6 km and for March-May.

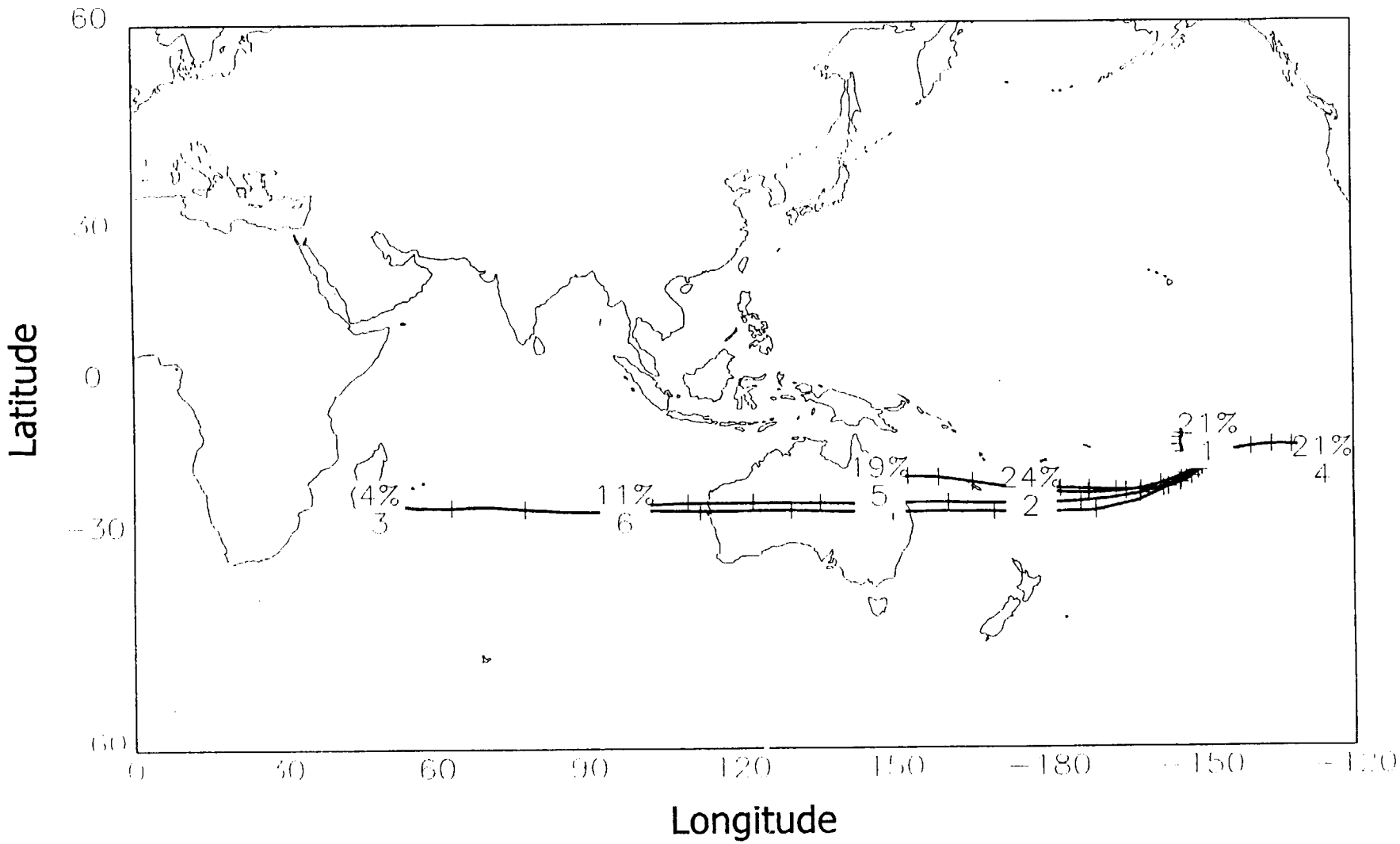

Figure 8b. Clusters of trajectories arriving at Tahiti at 6 km and for September-November.

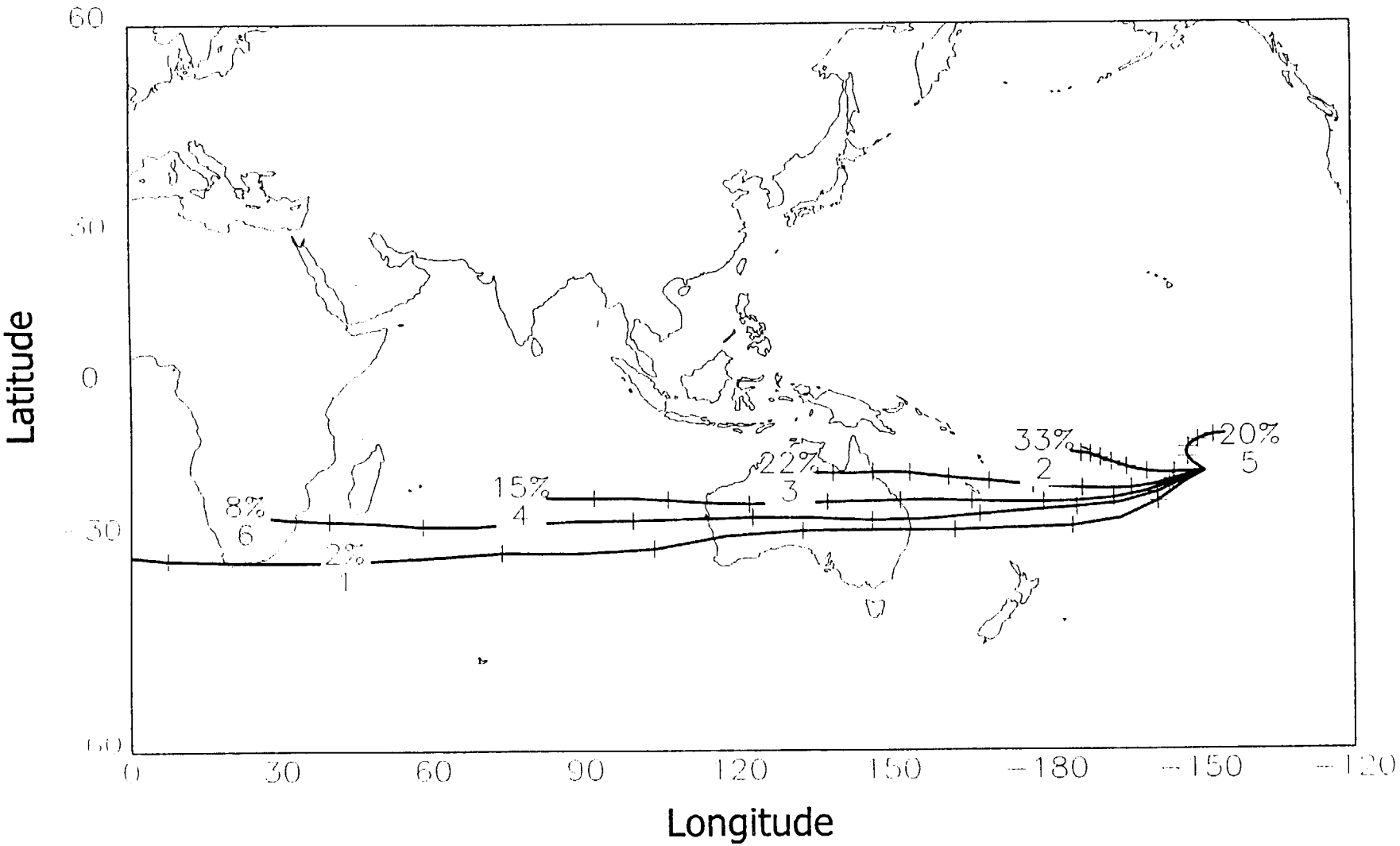

Figure 9. Clusters of trajectories arriving at Tahiti at for 13 km and for all seasons.

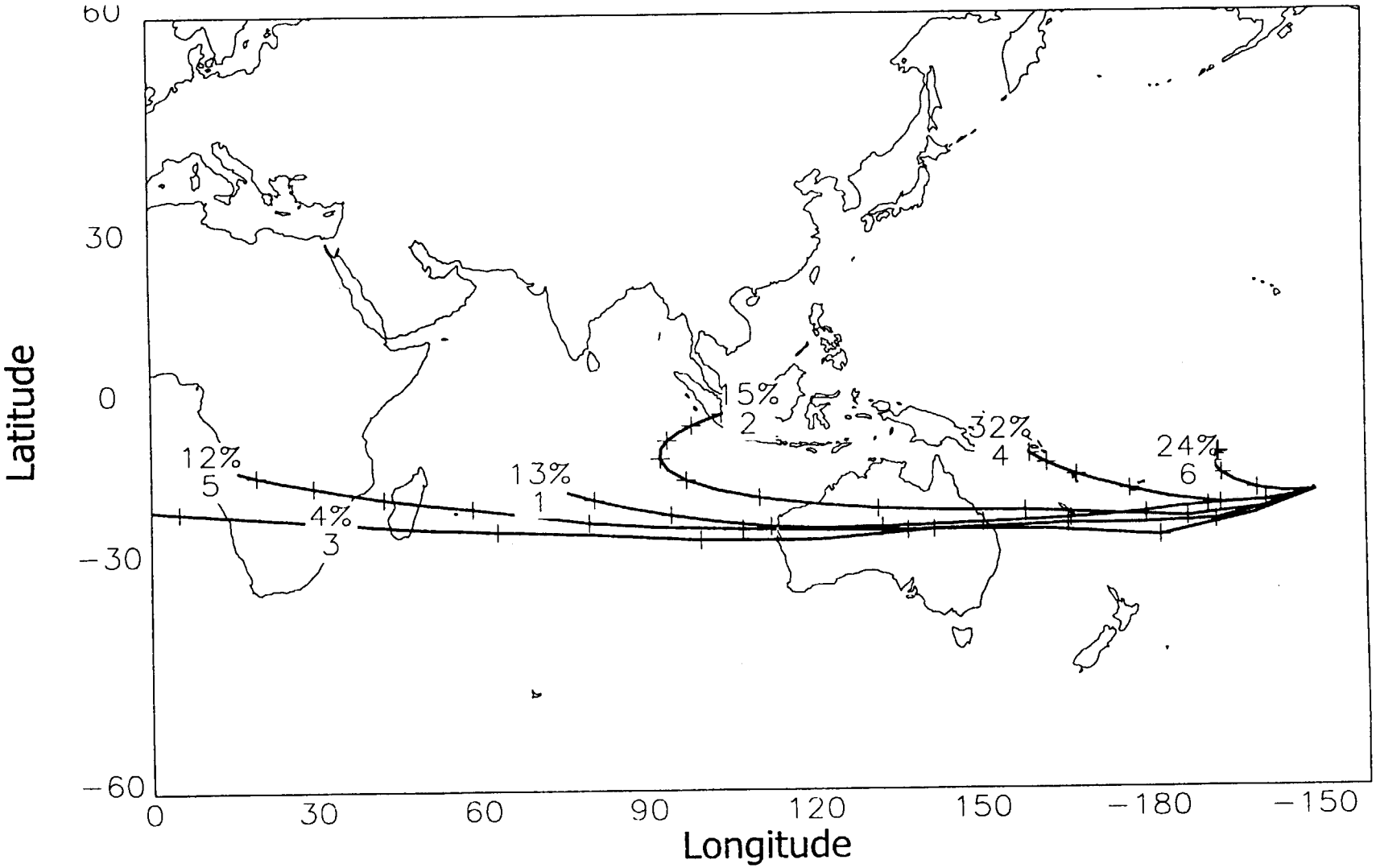

Figure 10. Clusters of trajectories arriving at the Galapagos at 1 km and for all seasons.

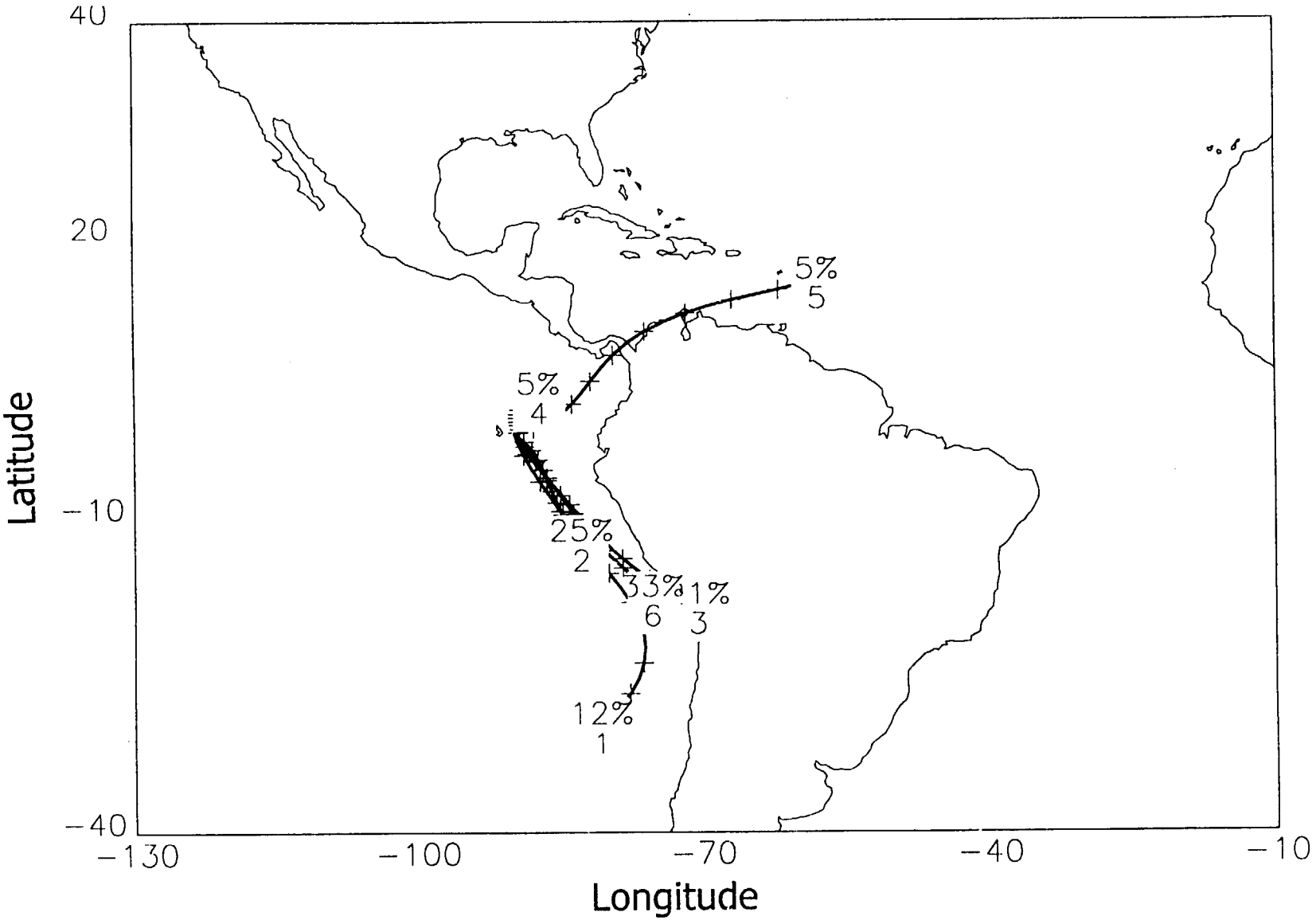

Figure 11a. Clusters of trajectories arriving at Galapagos at for 6 km and for December-February.

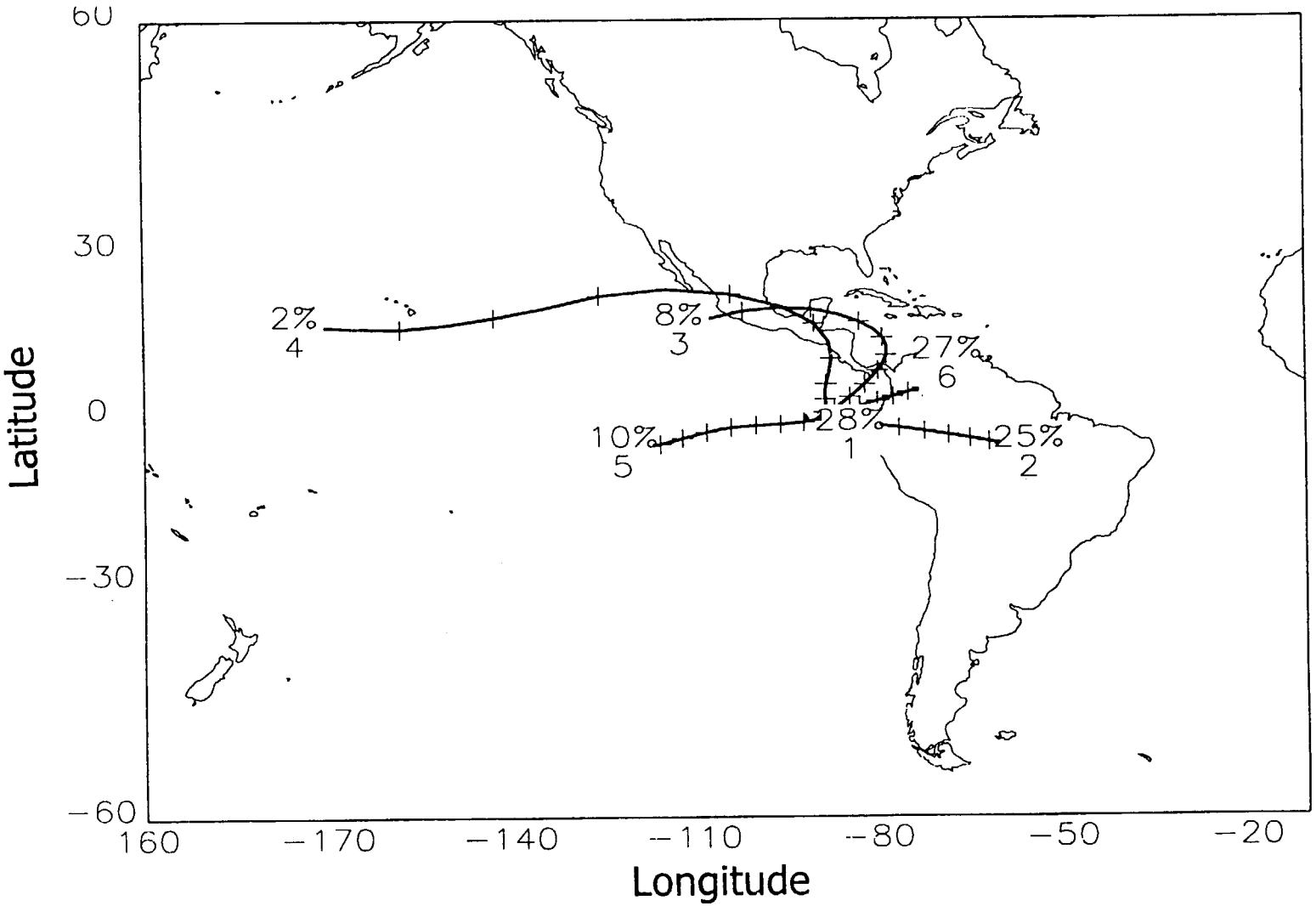

Figure 11b. Clusters of trajectories arriving at the Galapagos at for 6 km and for June-August.

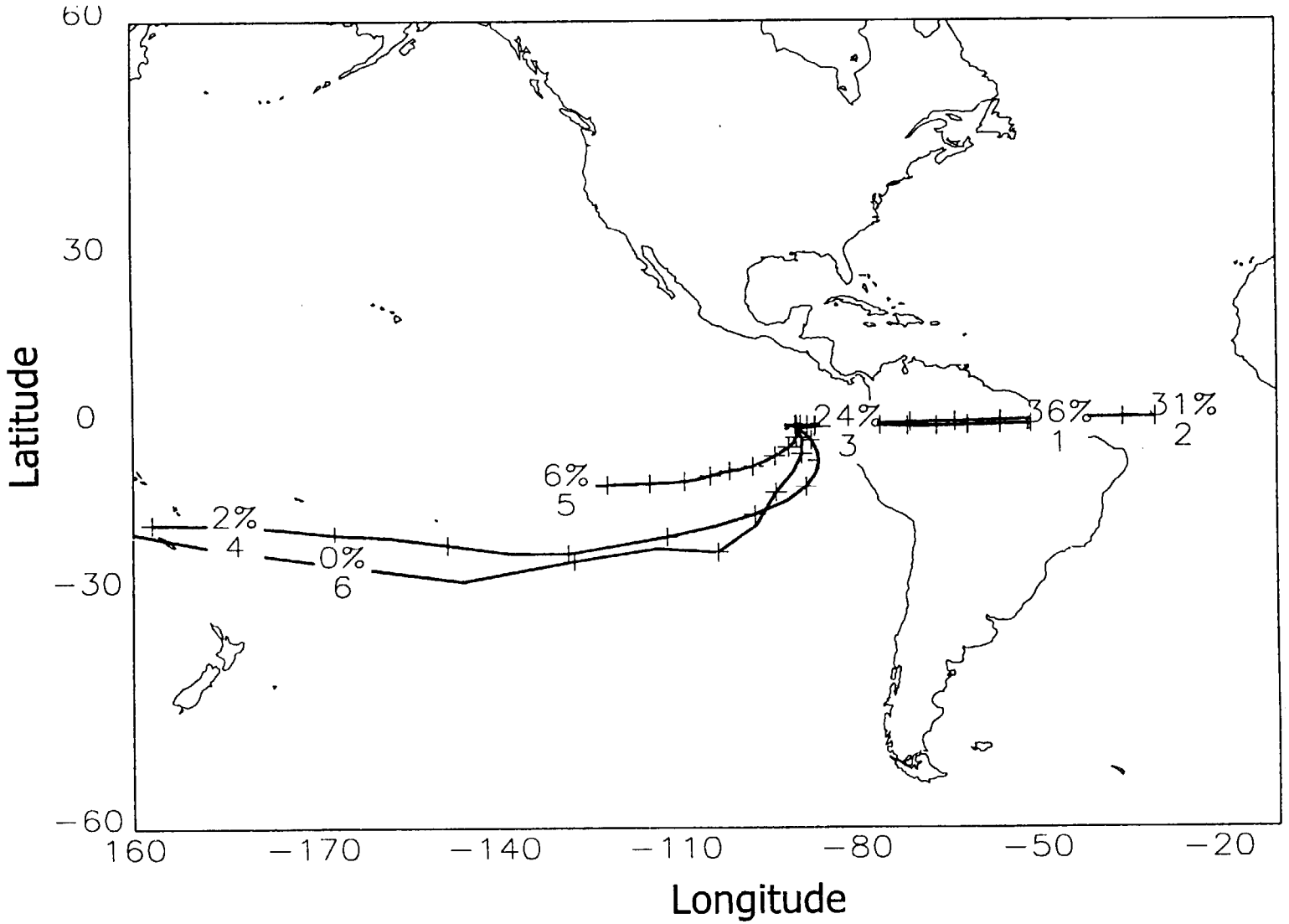

Figure 12. Clusters of trajectories arriving at the Galapagos at 13 km and for all seasons.

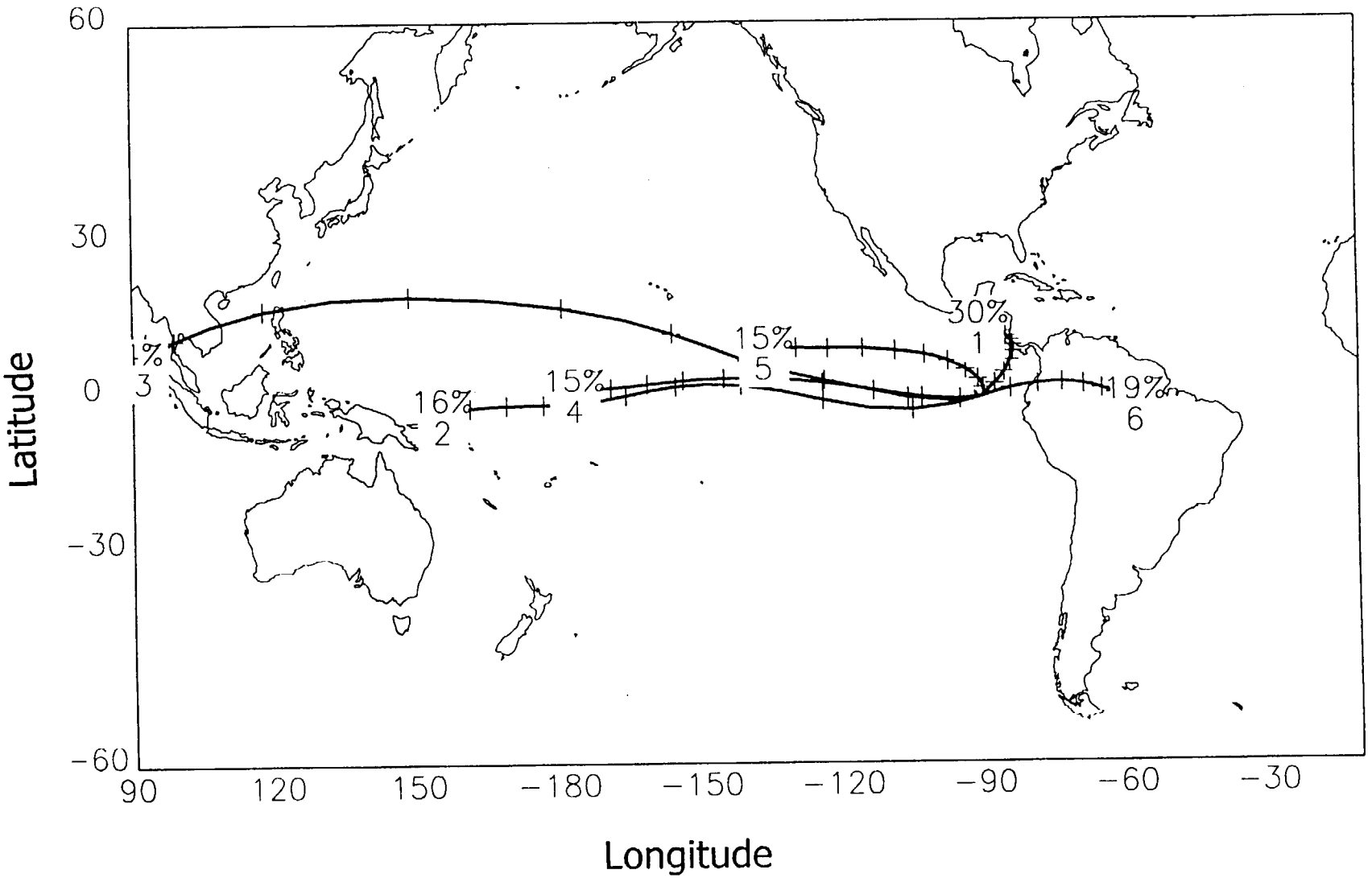

Figure 13. Ozone mixing ratio profile at Samoa on October 30, 1998. The thicker solid line is the ozone mixing ratio. The thinner line to the right is the air temperature and the thinner line to the left is the frost-point temperature.

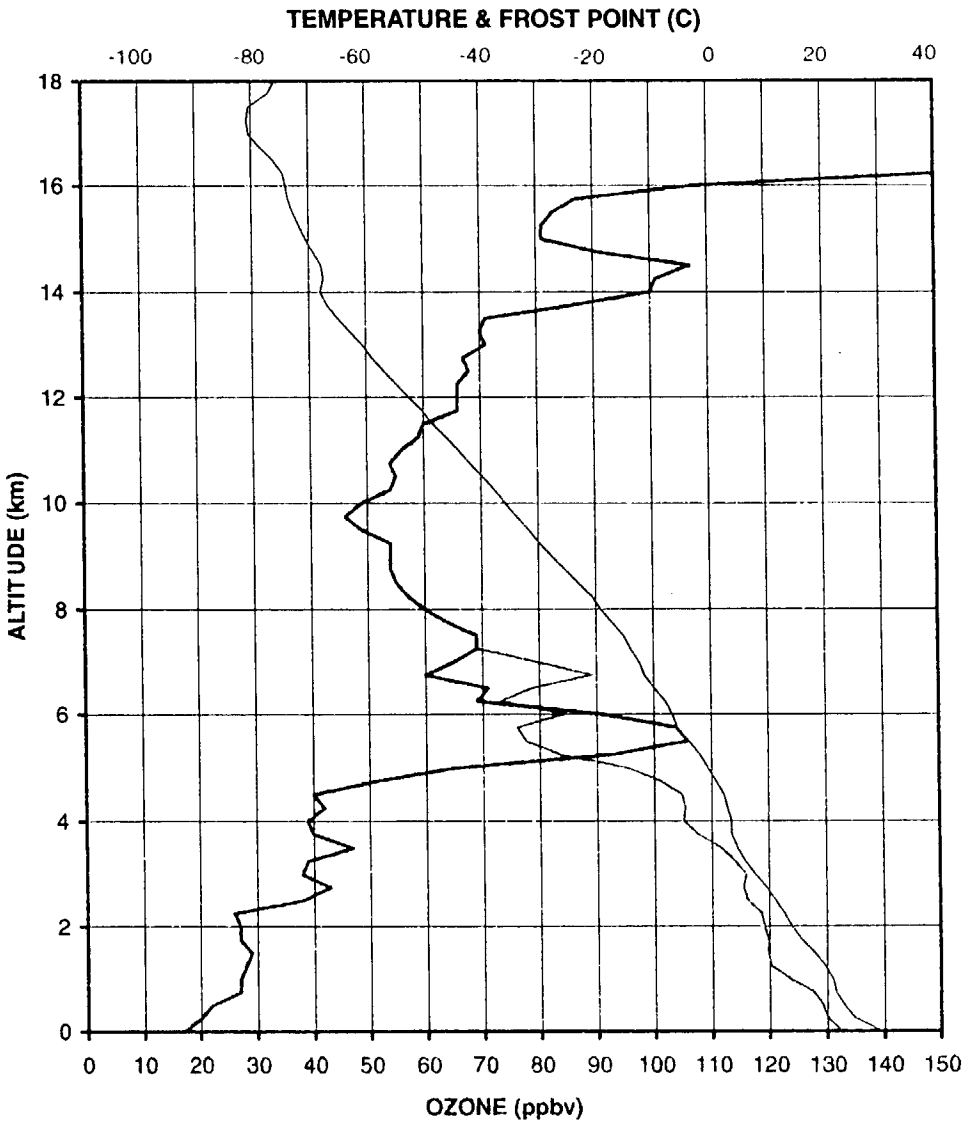

Figure 14. Trajectory to Samoa at 5 km on October 30, 1998 at 00Z

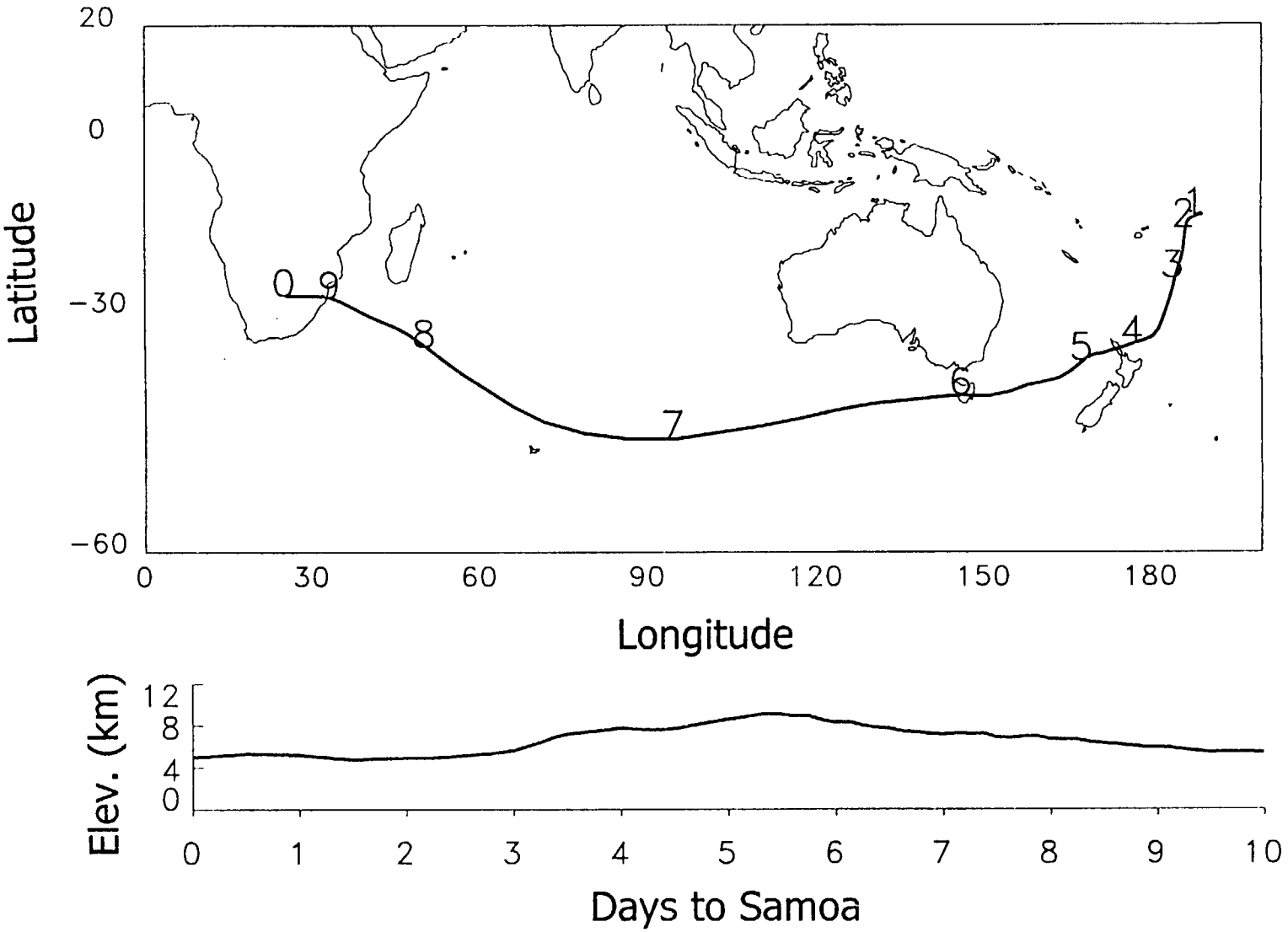

Figure 15. Ozone mixing ratio profiles at Samoa on a) October 2, 1997 and b) October 30, 1997.

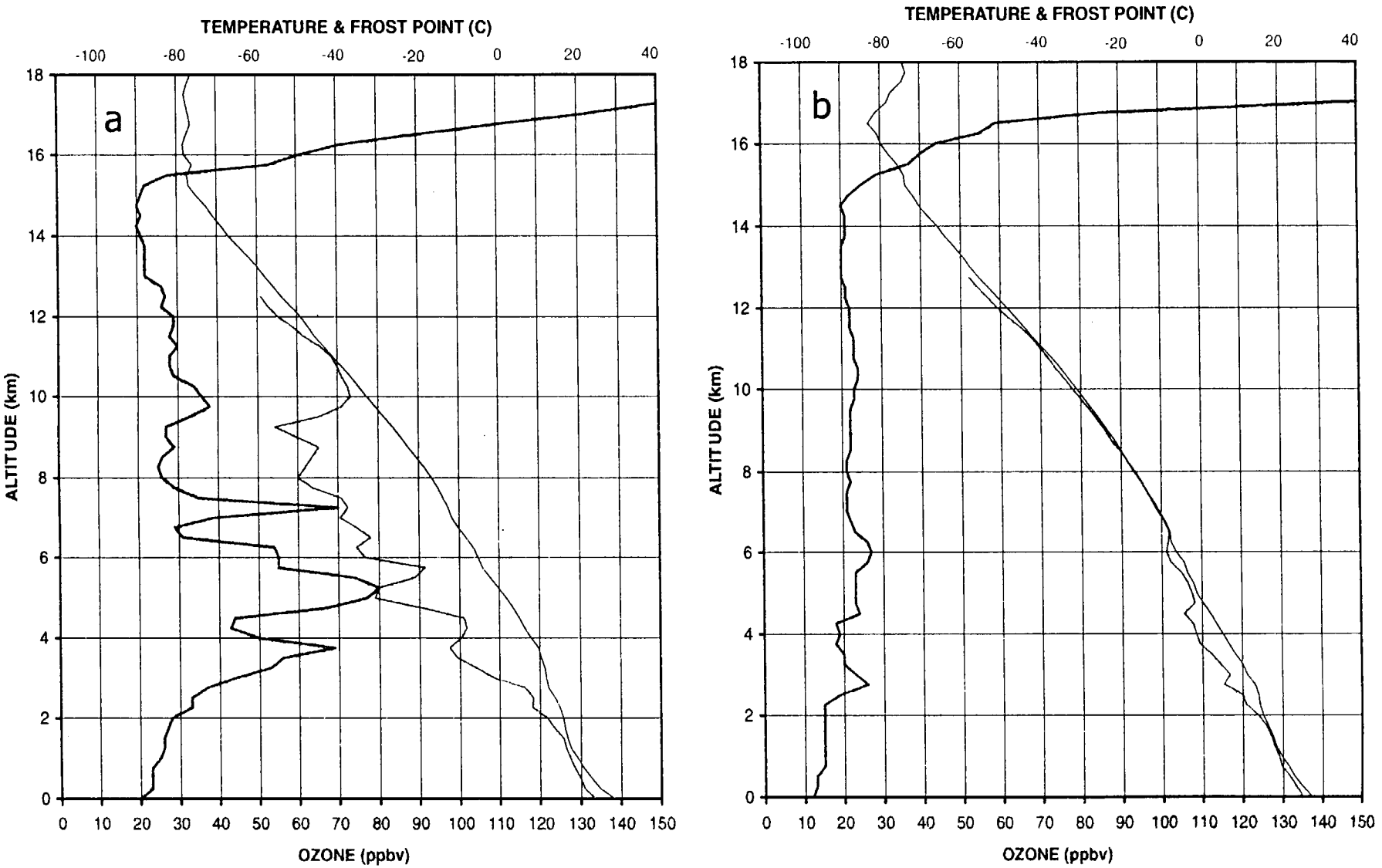

Figure 16a. Trajectory to Samoa at 5 km on October 2, 1997 at 00Z and 12Z.

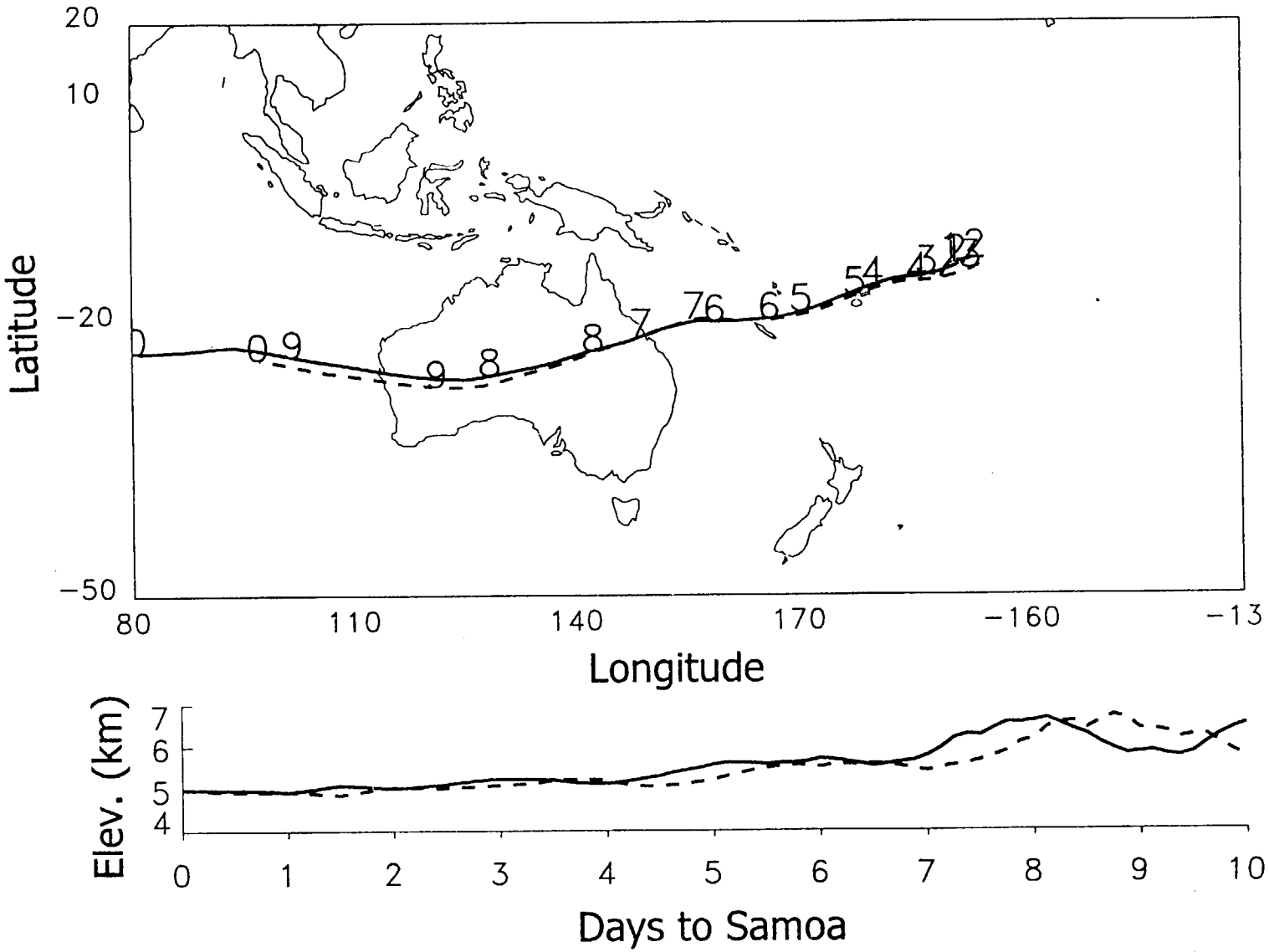

Figure 16b. Trajectory to Samoa at 5 km on October 31, 1997 at 00Z.

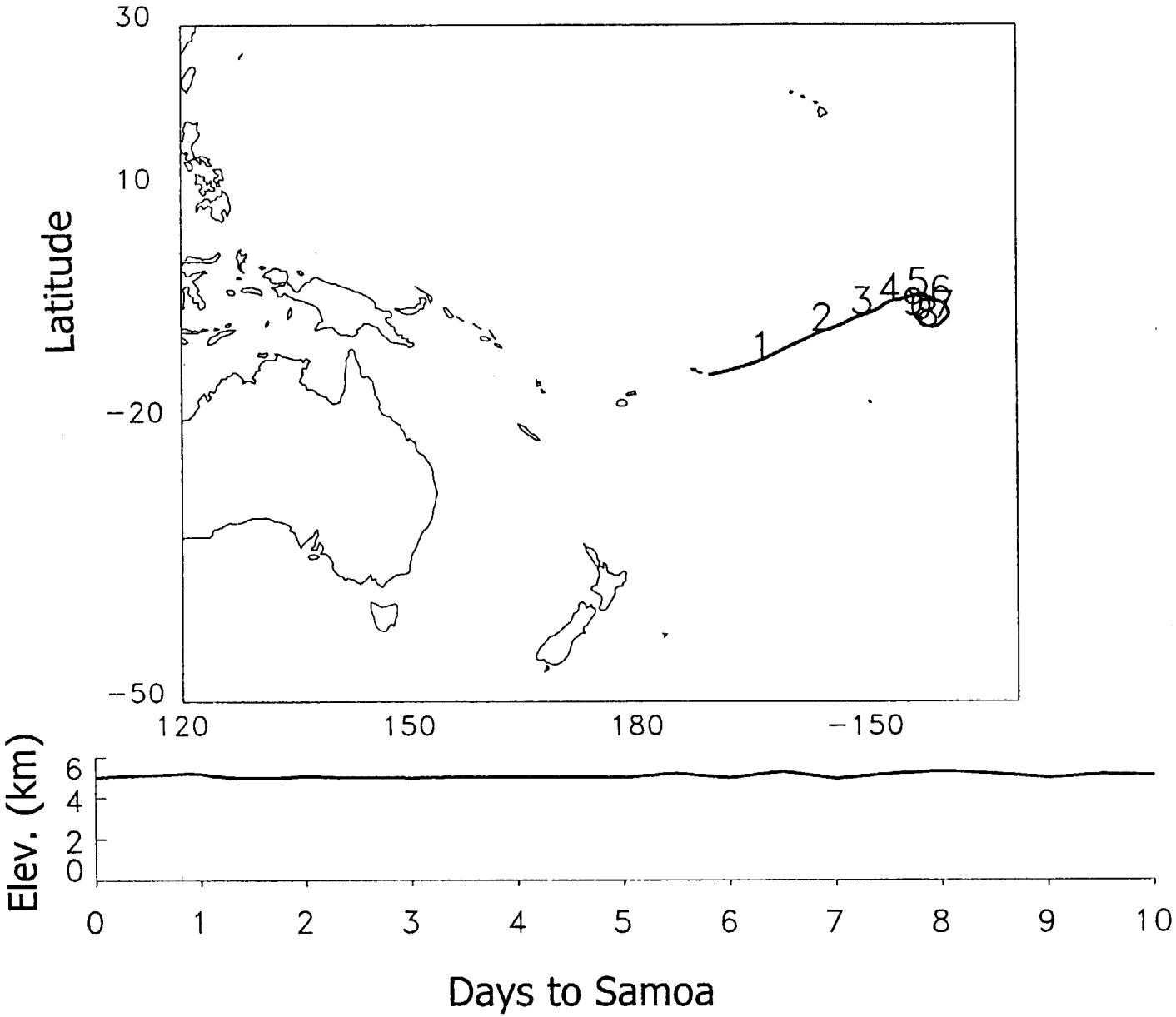

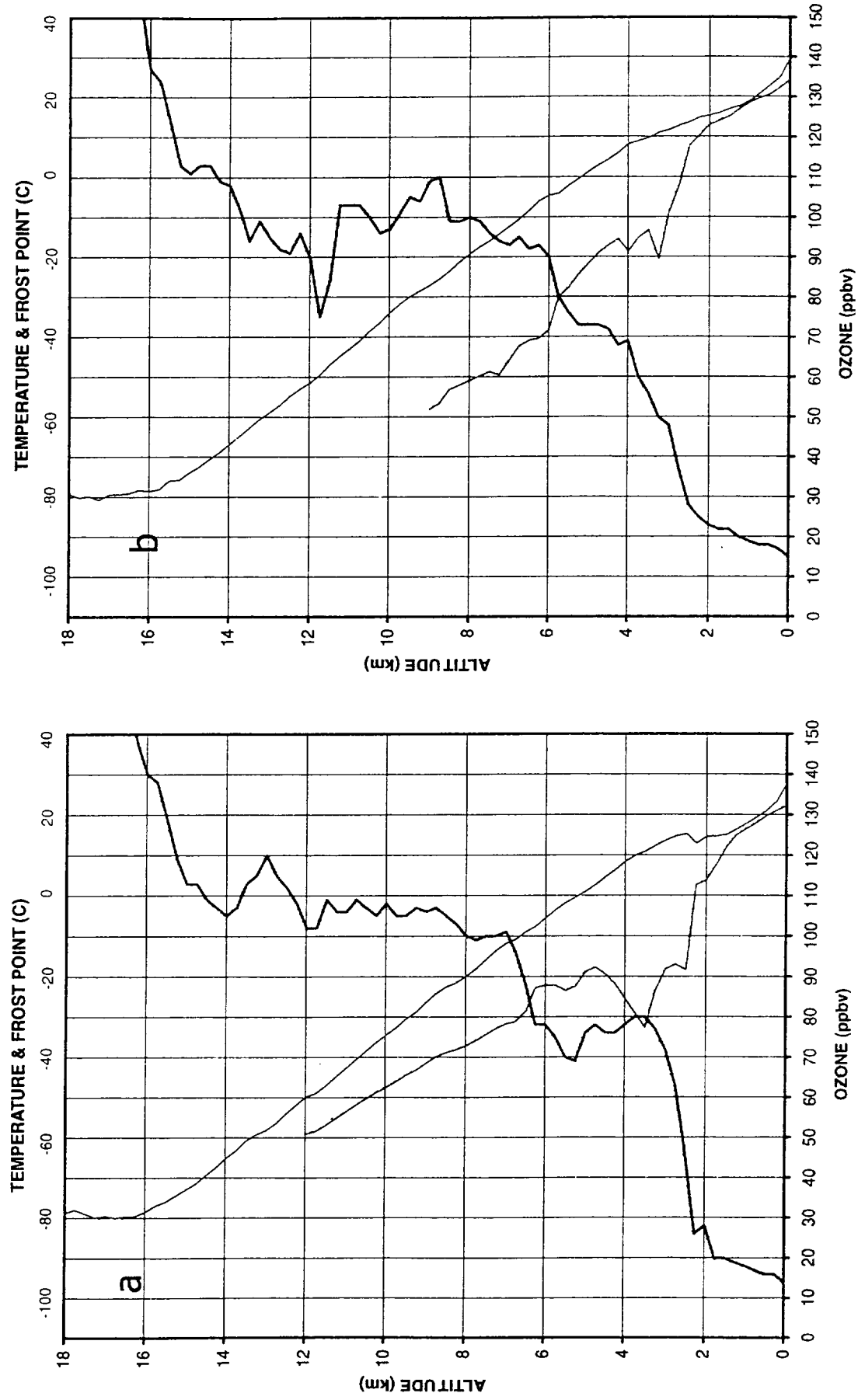

Figure 19. Ozone mixing ratio profile at a) Fiji on November 19, 1997 and b) Samoa on November 20, 1997.

Figure 17. Ozone mixing ratio profile at Tahiti on October 31, 1995.

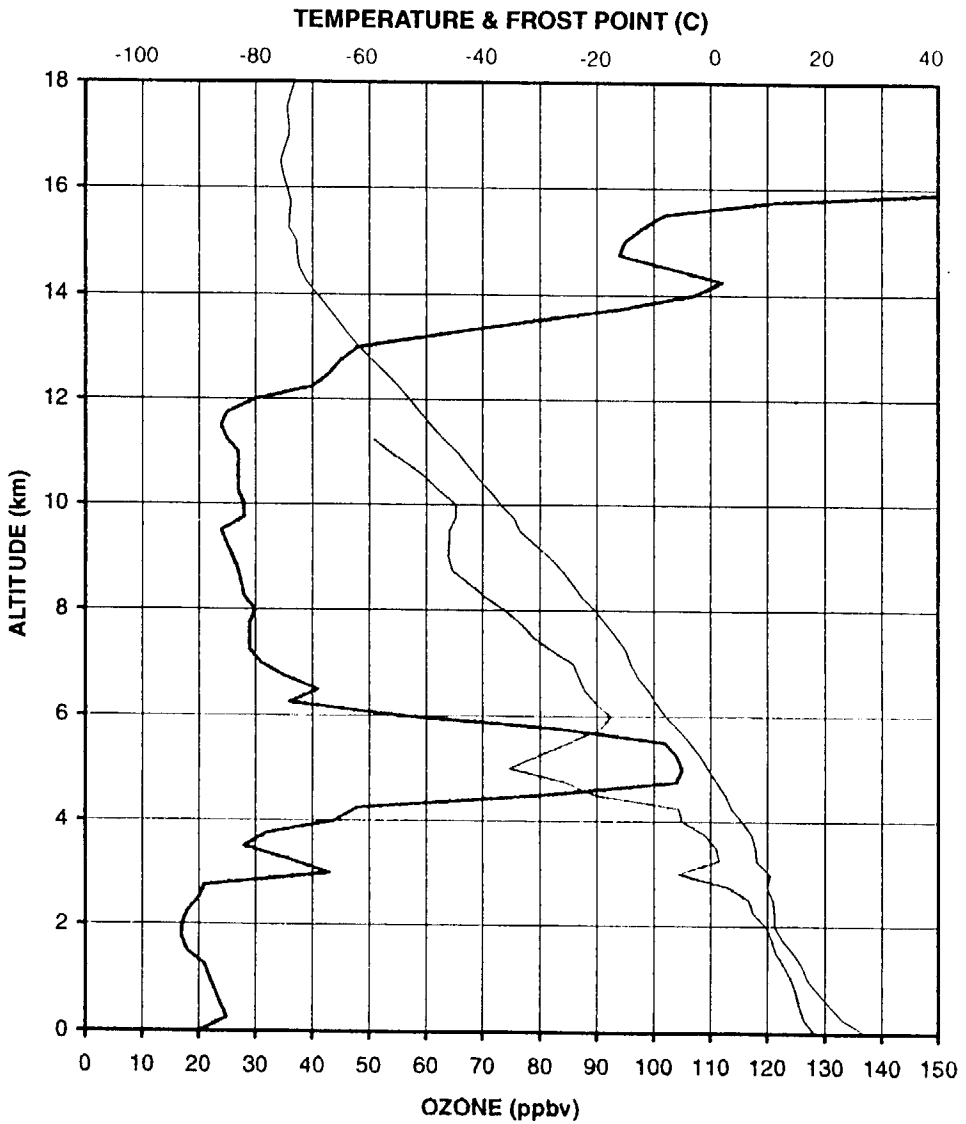

Figure 18. Trajectory to Tahiti at 5 km on November 1, 1995 at 00Z and 12Z.

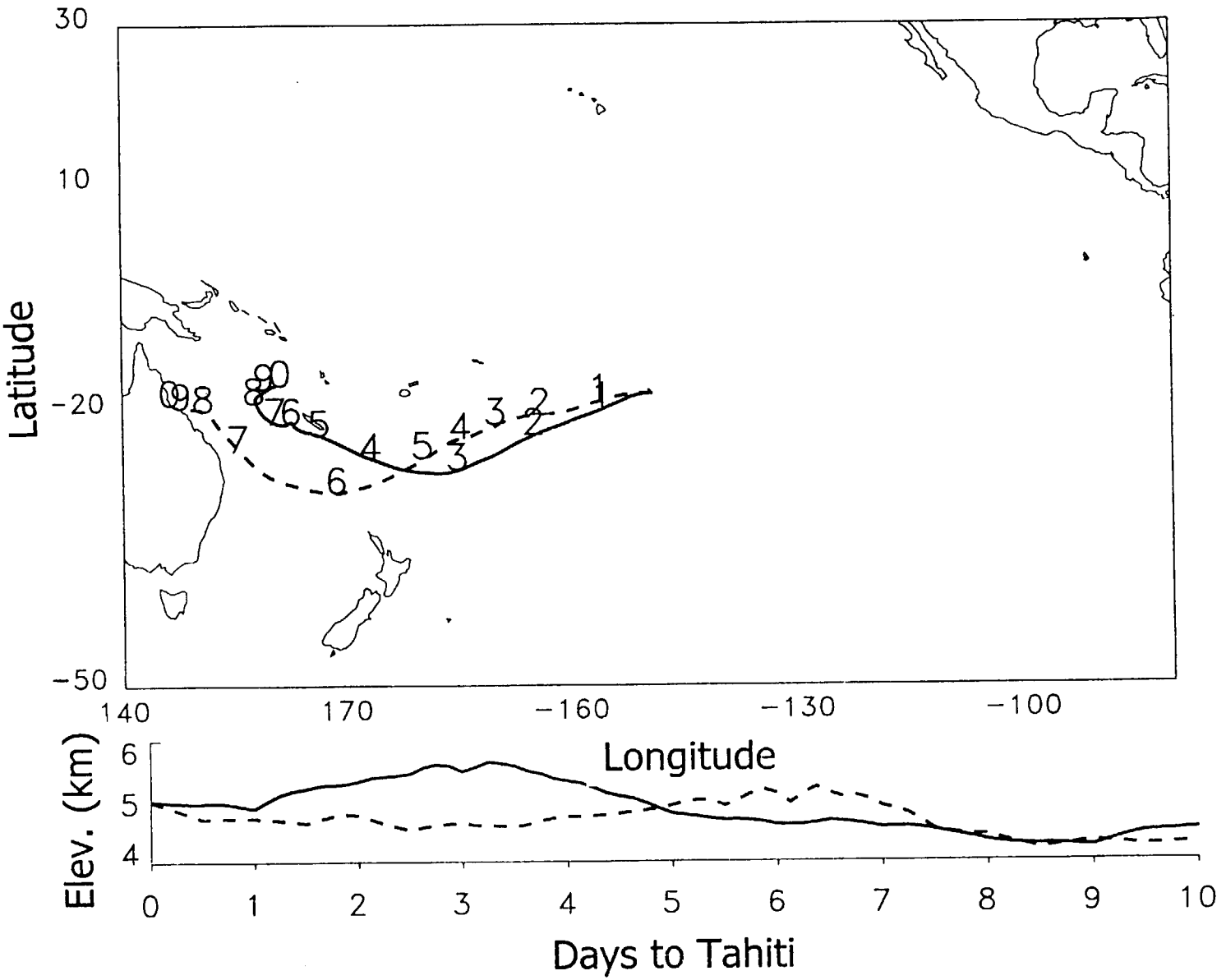

Figure 19. Ozone mixing ratio profile at a) Fiji on November 19, 1997 and b) Samoa on November 20, 1997.

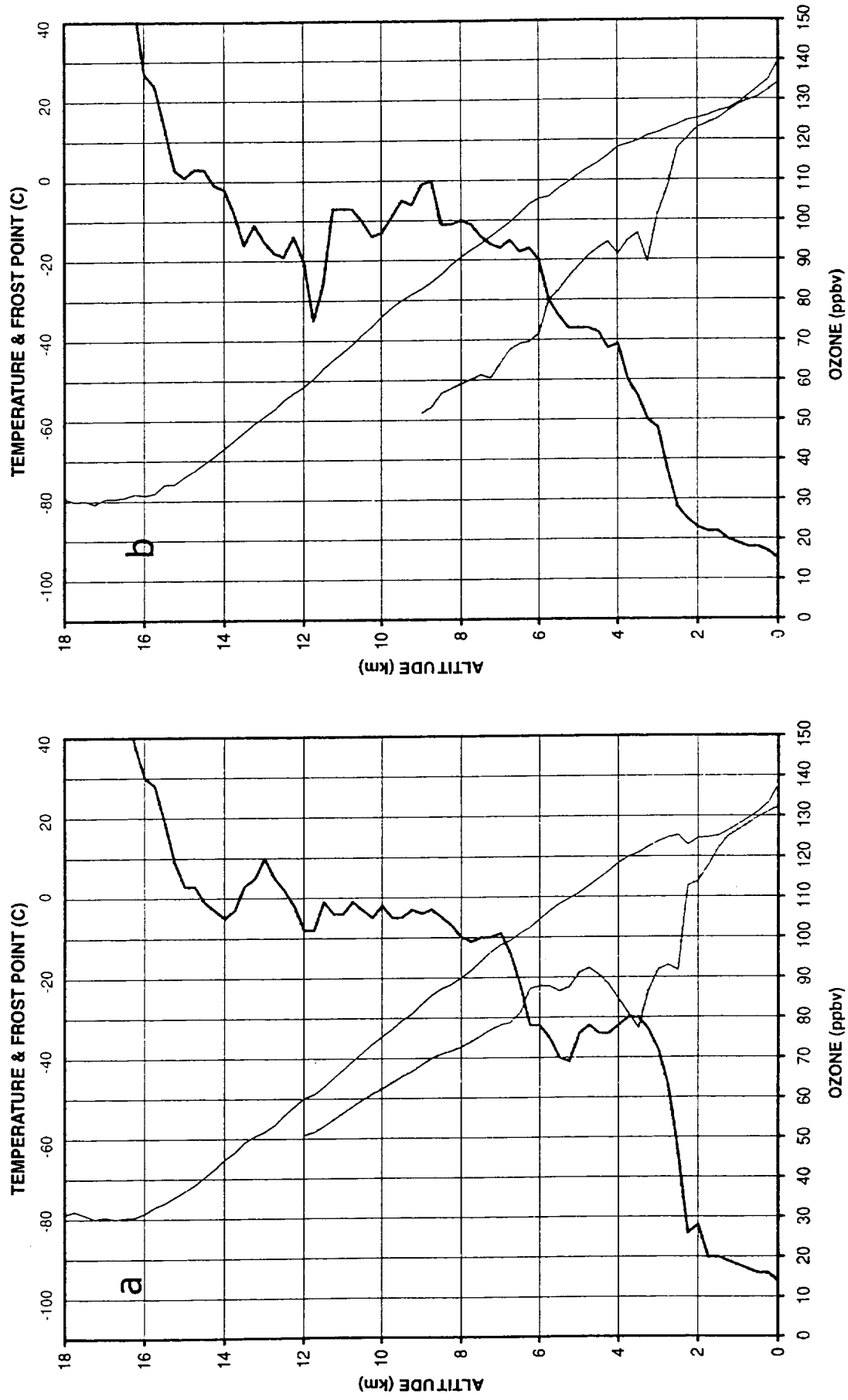

Figure 20a. Trajectory to Fiji at 8 km on November 20, 1997 at 00Z and 12Z.

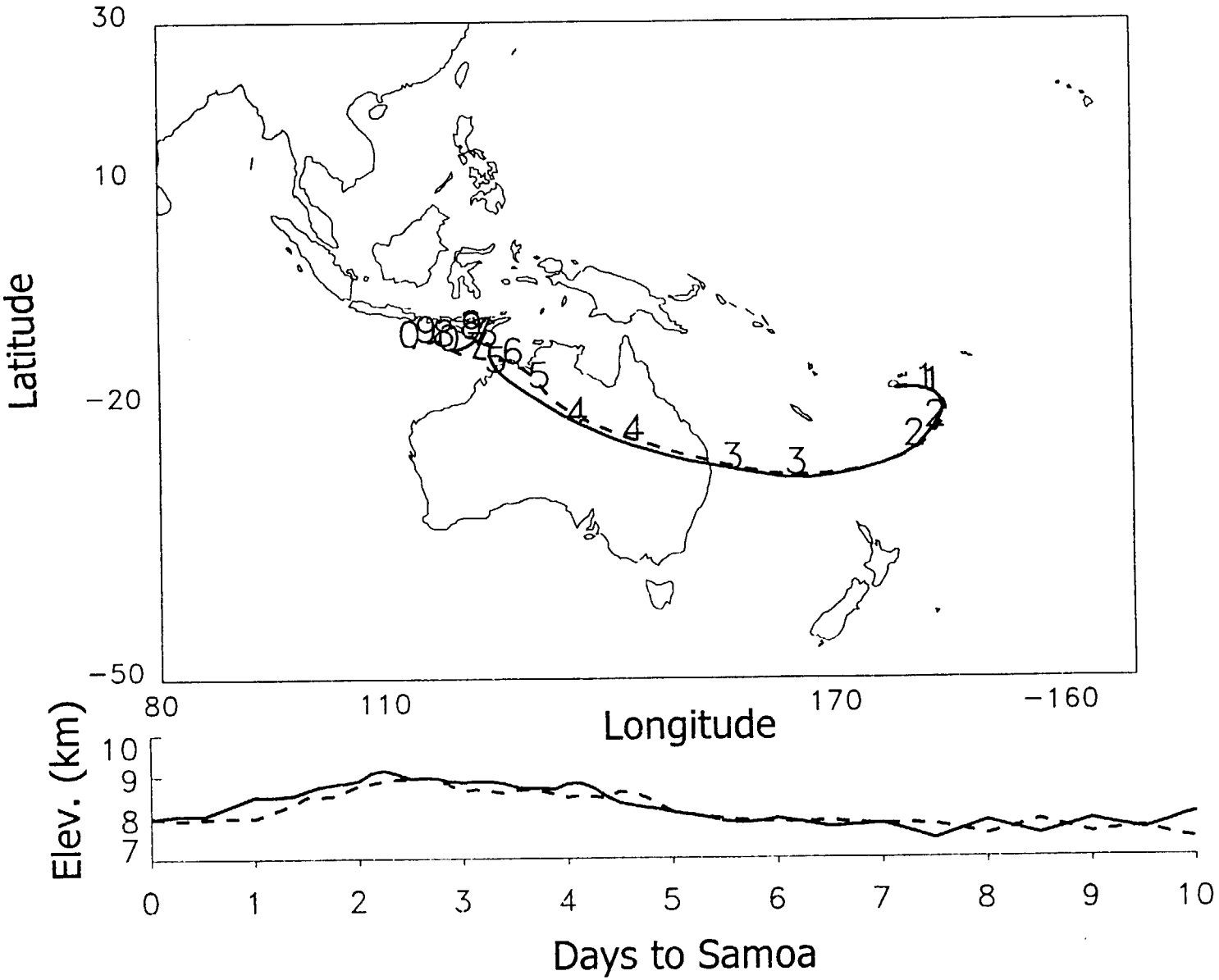

Figure 20b. Trajectory to Samoa at 6 km on November 20, 1997 at 00Z and 12Z.

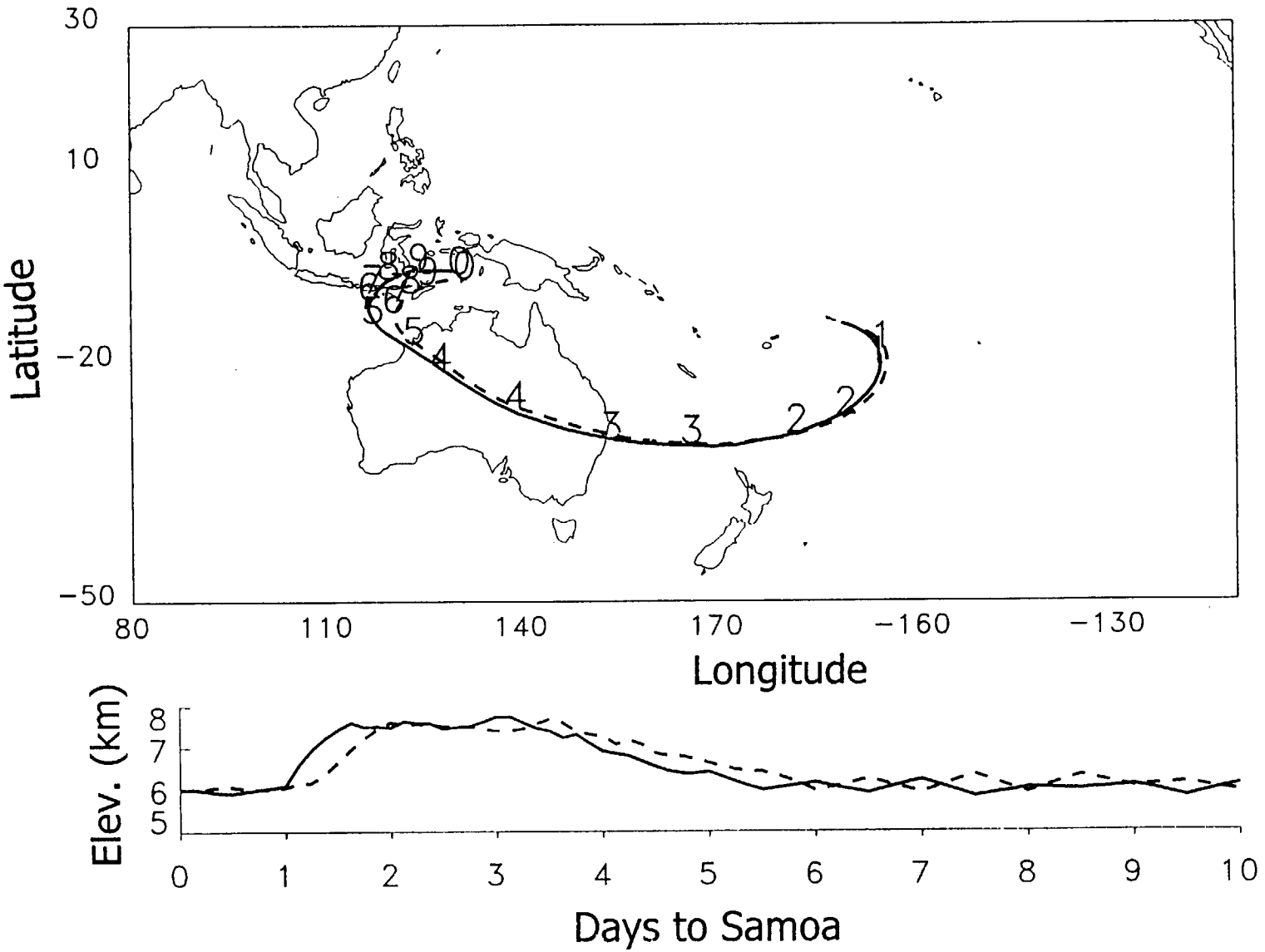

Figure 20c. Trajectory to Samoa at 10 km on November 21, 1997 at 00Z and 12Z.

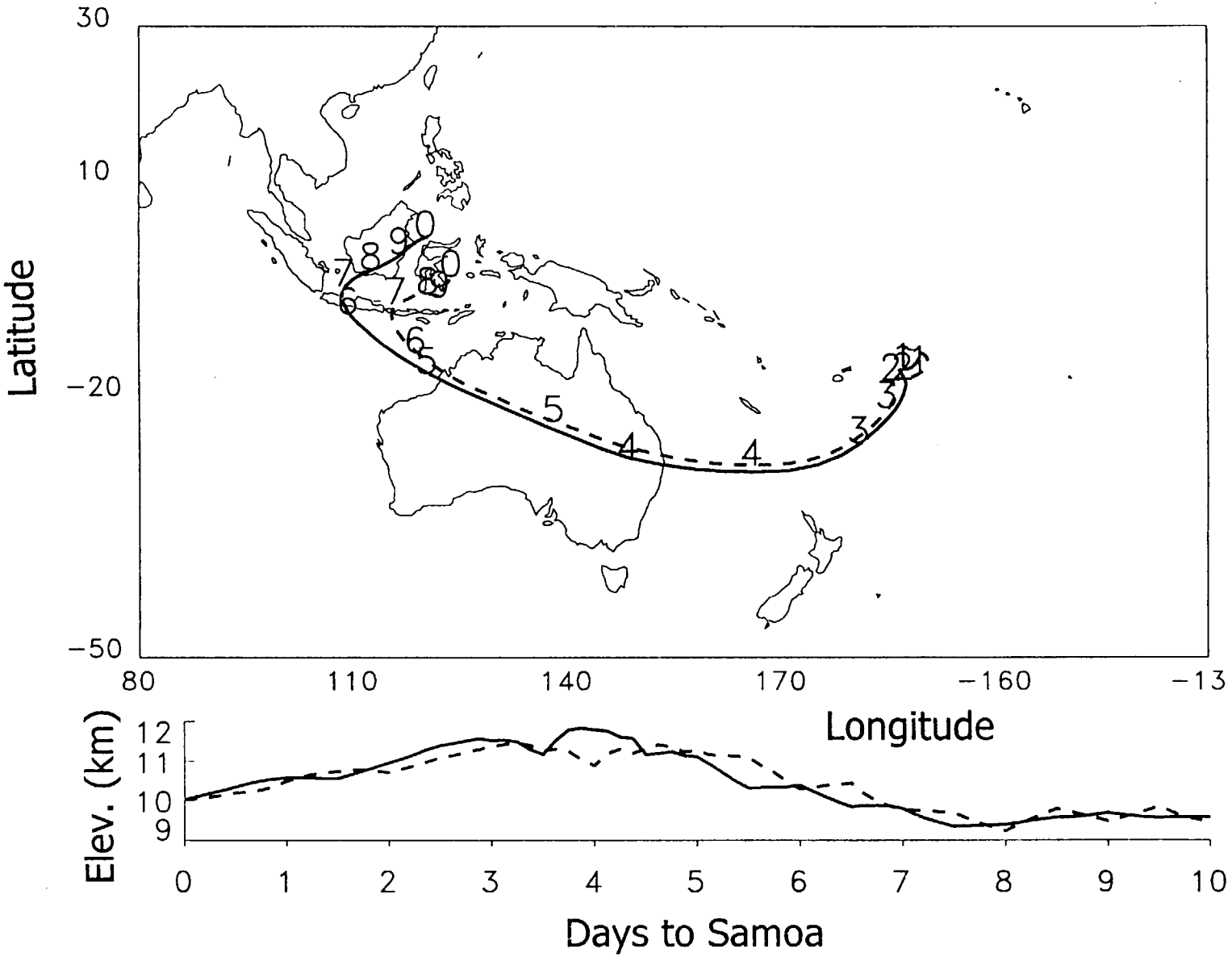

Figure 20d. Trajectory to Fiji at 8 km on November 23, 1997 at 00Z and 12Z.

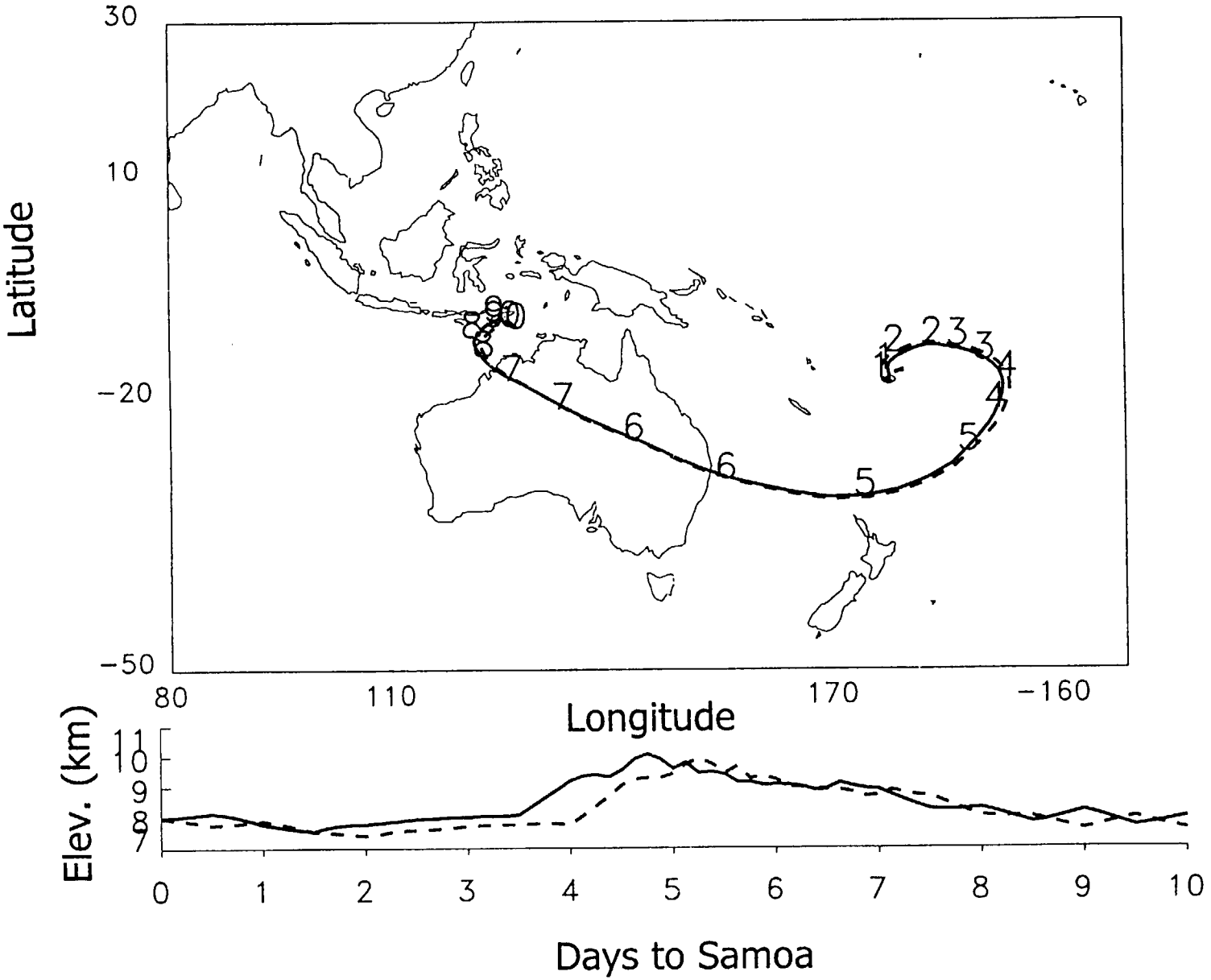

Figure 21. Ozone mixing ratio profile at Samoa on February 20, 1999.

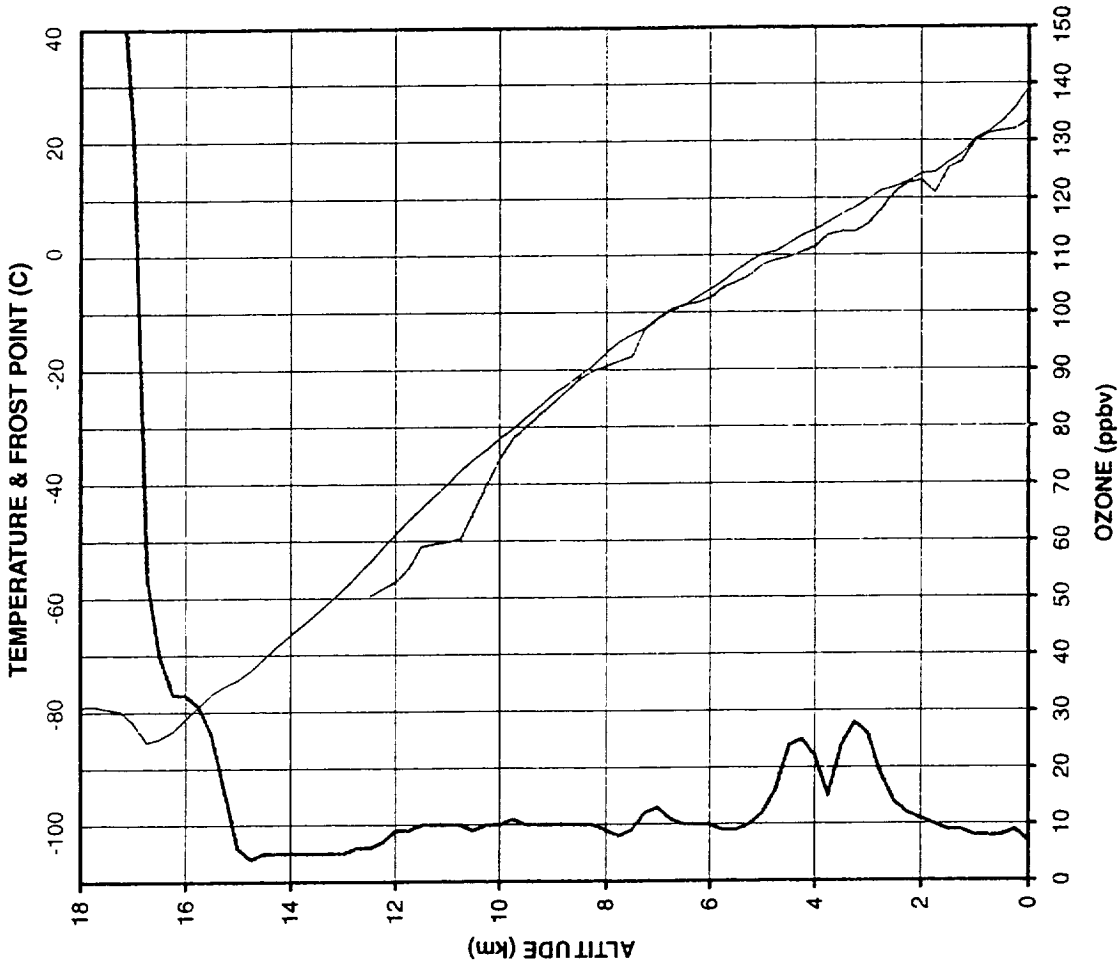

Figure 22. Trajectory to Samoa at 13 km on February 20, 1999 at 00Z and 12Z.

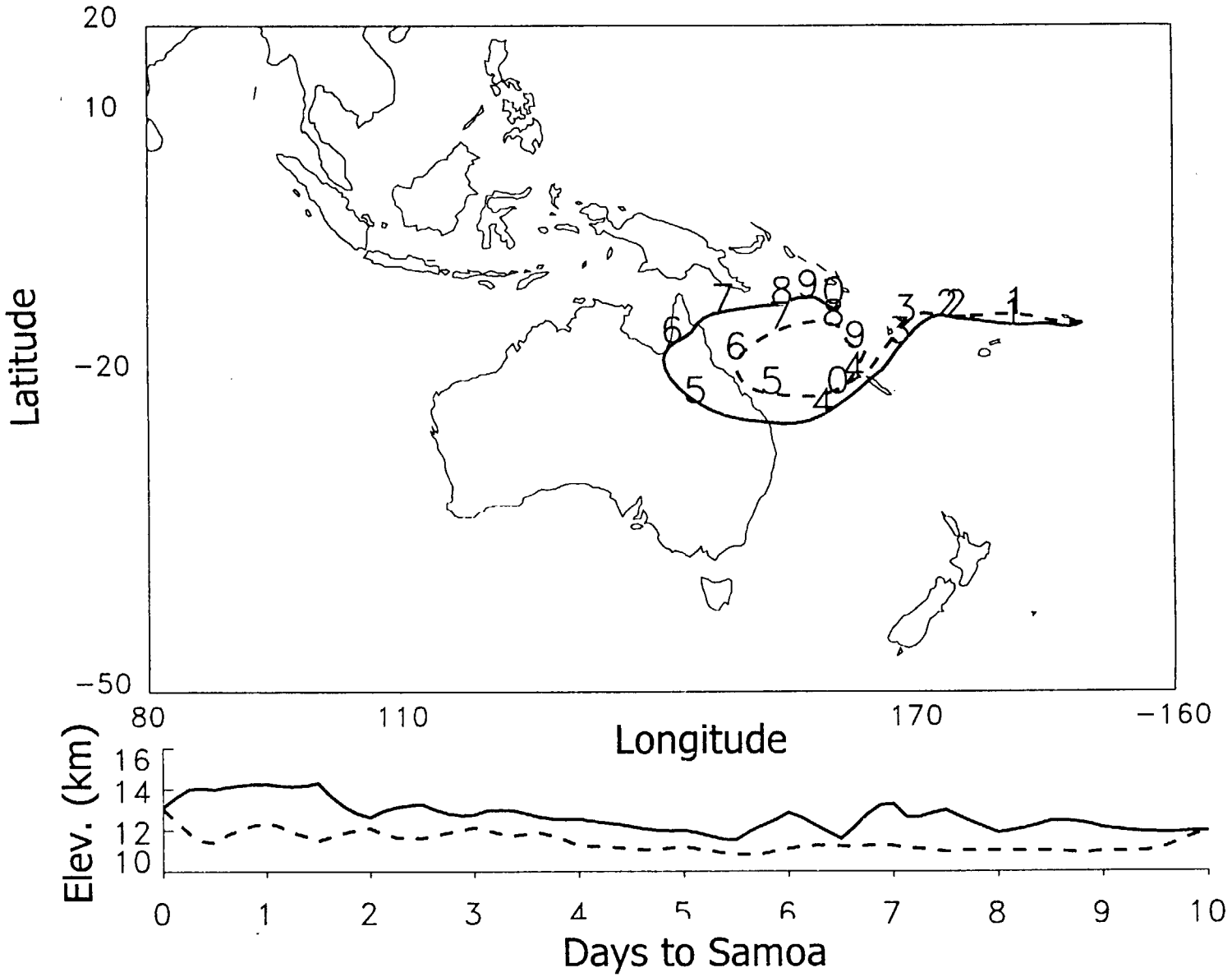

Figure 23. Ozone mixing ratio profile at the Galapagos on October 9, 1999 at 15Z. The thicker solid line is the ozone mixing ratio. The thinner line to the right is the air temperature and the thinner line to the left is the frost-point temperature.

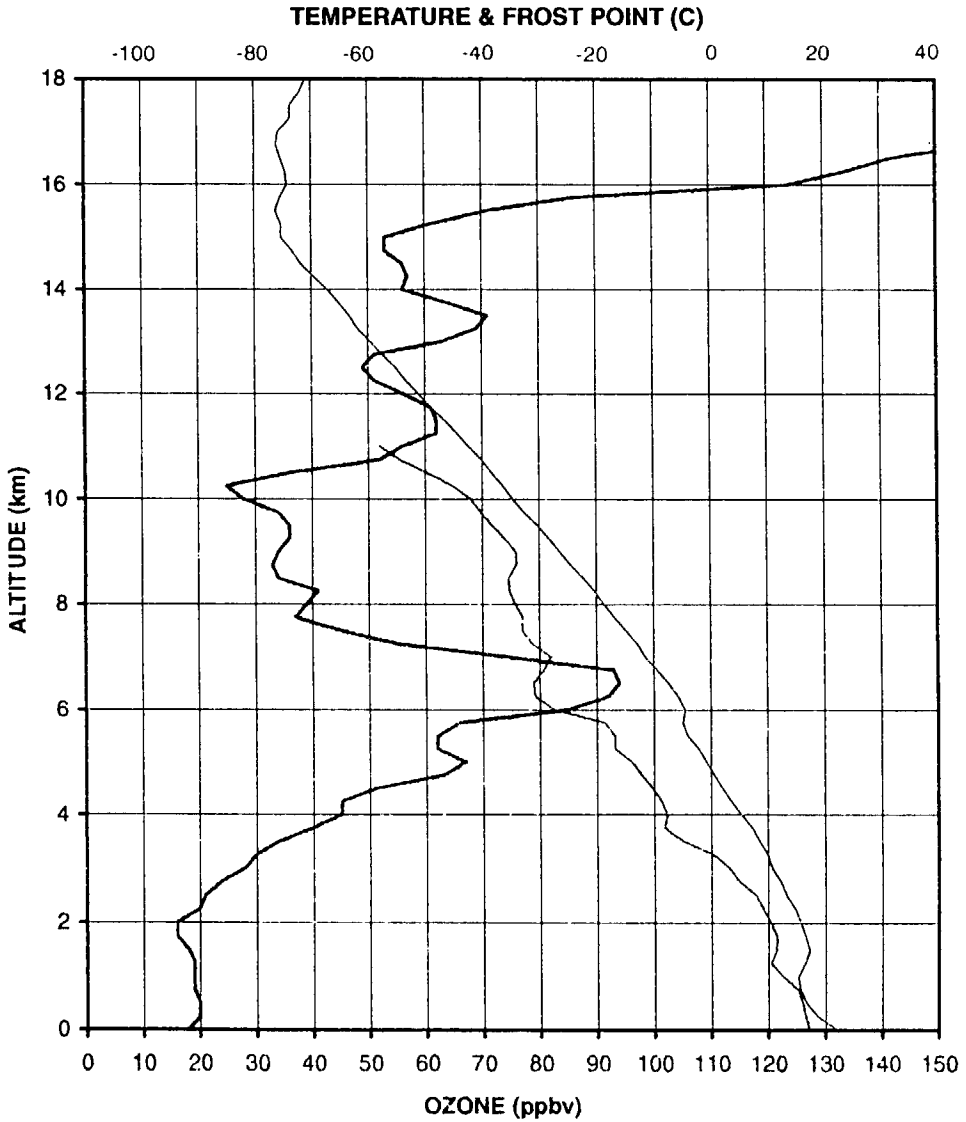

Figure 24. Trajectory to the Galapagos at 6 km on October 10, 1999 at 00Z.

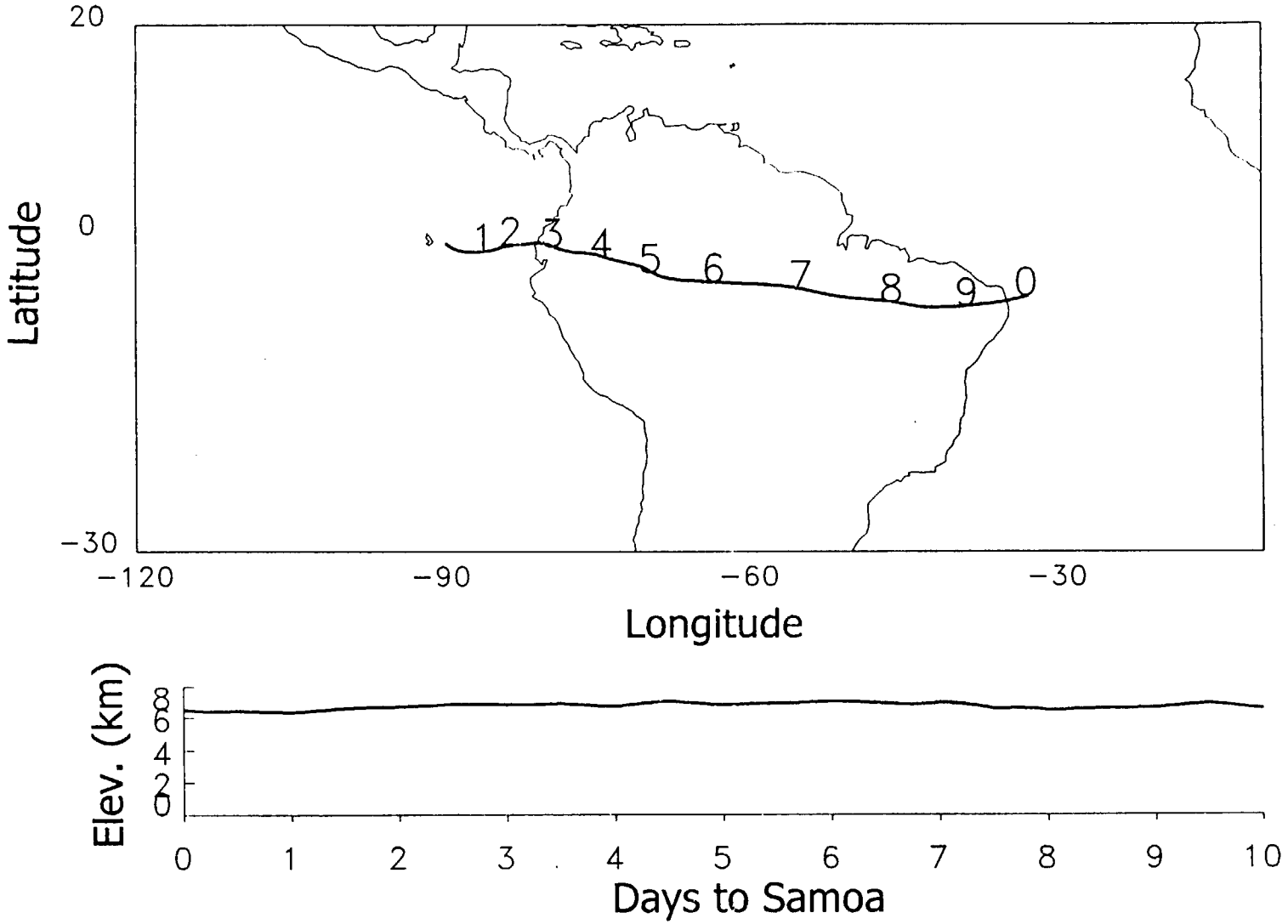

Figure 25. Ozone mixing ratio profiles at the Galapagos on a) March 25, 1999 and b) April 4, 1998.

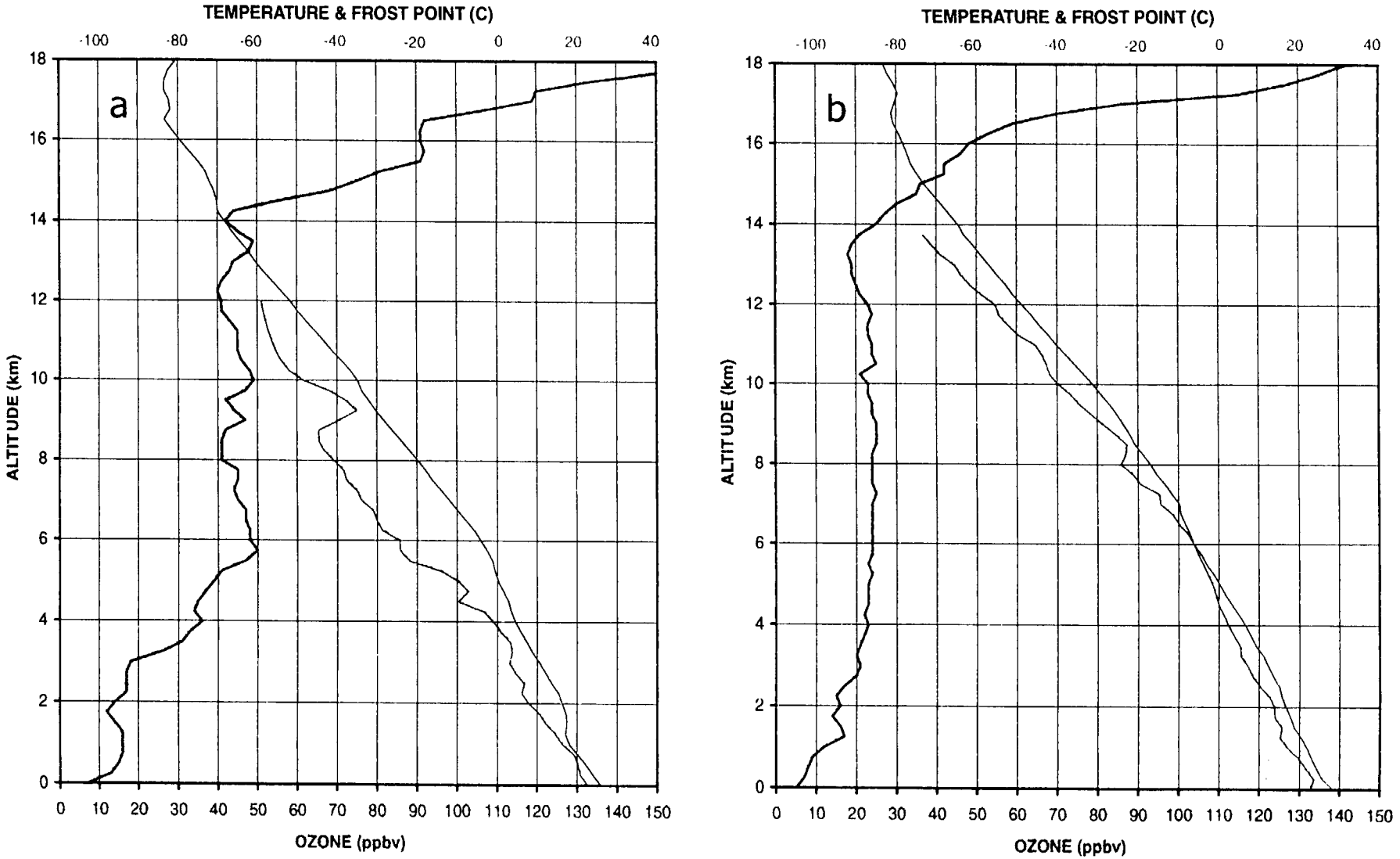

Figure 26a. Trajectories to the Galapagos at 6 km on March 25, 1999 at 12Z.

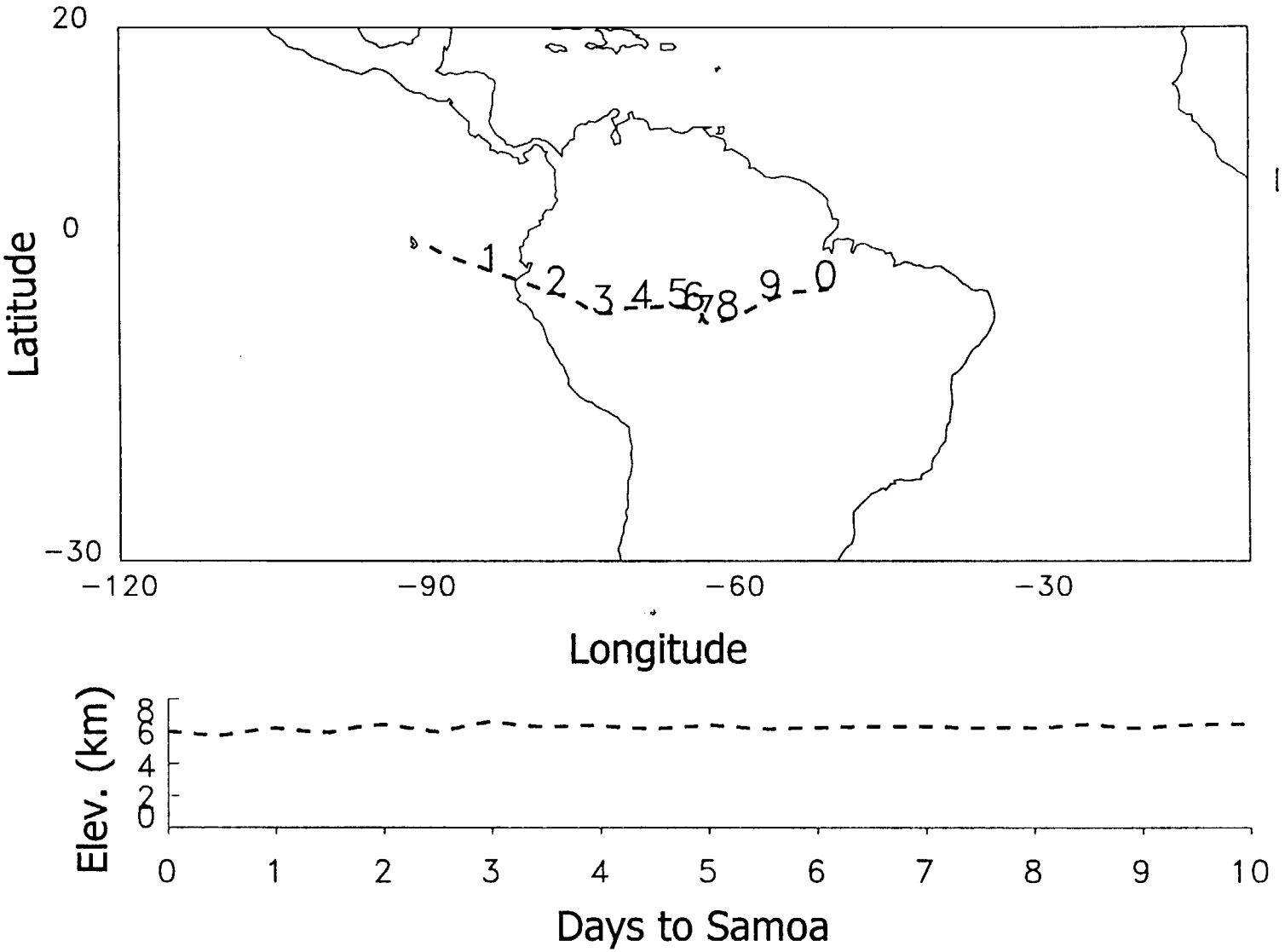

Figure 26b. Trajectories to the Galapagos at 6 km on April 4, 1998 at 12Z.